

Supporting Information

pH reversibly activatable NIR photothermal/photodynamic-in-one agent integrated with renewable nanoimplant for image-guided precision phototherapy

Xu Zhao,^{a,b,c,*} Kai-Chao Zhao,^{c,d} Li-Jian Chen,^{a,b,c} Yu-Shi Liu,^c Jia-Lin Liu,^{c,d} and Xiu-Ping Yan^{a,b,c,d,*}

¹State Key Laboratory of Food Science and Technology, Jiangnan University, Wuxi 214122, China

² International Joint Laboratory on Food Safety, Jiangnan University, Wuxi 214122, China

³ Institute of Analytical Food Safety, School of Food Science and Technology, Jiangnan University, Wuxi 214122, China

⁴ Key Laboratory of Synthetic and Biological Colloids, Ministry of Education, School of Chemical and Material Engineering, Jiangnan University, Wuxi, 214122, China

*Corresponding authors. E-mail: zhaoxu2017@jiangnan.edu.cn (Xu Zhao);
xpyan@jiangnan.edu.cn (Xiu-Ping Yan)

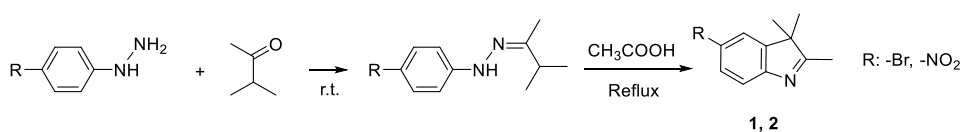
Supplementary Methods

Chemicals and materials. All reagents were of at least of analytical grade and used as supplied without further purification unless otherwise noted. 4-Bromophenylhydrazine hydrochloride (99%), methyl isopropyl ketone (99%), 4-(bromomethyl) benzoic acid methyl ester (98%), 4-nitrophenylhydrazine hydrochloride (96%), biotin (98%), chloroacetyl chloride (98%), Ga₂O₃ (99.99%), Zn(NO₃)₂·6H₂O (99.99%), Cr(NO₃)₃·9H₂O (99.99%), Yb(NO₃)₃·5H₂O (99.9%), Er(NO₃)₃·5H₂O (99.9%), (3-aminopropyl) triethoxysilane (APTES, 99%), 1-ethyl-3-(3-dimethylaminopropyl) carbodiimide hydrochloride (EDC·HCl, 98%), *N*-hydroxysuccinimide (NHS, 98%), *N,N*-diisopropylethylamine (DIPEA, 99%) were purchased from Aladdin (Shanghai, China). Indocyanine Green (90%) and 1,3-diphenylisobenzofuran (DPBF, 97%) were obtained from J&K Scientific (Beijing, China). Biotin functionalized polyethylene glycol (2K) (PEG-Biotin) was provided by Xi'an Ruixi Biological Tehnology Co. Ltd. (Xi'an, China). 4',6-diamidino-2-phenylindole (DAPI), 3-(4,5-Dimethyl-thiazol-2-yl)-2,5-diphenyltetrazolium bromide (MTT), Calcein acetoxymethyl ester (Calcein-AM) and propidium iodide (PI) were bought from Sigma-Aldrich Co. LLC (Shanghai, China). Cetyltrimethylammonium bromide (CTAB, 99%), GeO₂ (99.99%), acetate (99.5%), diethyl ether, NH₃·H₂O, K₂CO₃, NaOH, ethanol (EtOH), acetonitrile (CH₃CN), dichloromethane (CH₂Cl₂), *N,N*-dimethylformamide (DMF) and other reagents and solvents were supplied by Sinopharm Chemical Reagent Co., Ltd (Shanghai, China). Dulbecco's modified Eagle's high glucose medium (DMEM), fetal bovine serum (FBS), penicillin-streptomycin and other consumables for cell culture were purchased from Dingguo Biotechnology Co. (Beijing, China). High-purity water (Wahaha, Hangzhou Wahaha Group Co. Ltd., Hangzhou, China) was used throughout all experiments. All the glassware was soaked in aqua regia (HCl/HNO₃ = 3/1, v/v) and thoroughly rinsed with high-purity water before used.

Instrumentation and characterization. ¹H and ¹³C nuclear magnetic resonance spectra (¹H

NMR and ^{13}C NMR) were carried out on a Bruker AVANCE III HD 400 MHz spectrometer with tetramethyl silane as an internal standard (Bruker, Switzerland). Mass spectra were acquired on a QTRAP 4500 (AB SCIEX, USA). Fourier transform infrared (FT-IR) spectra were recorded on a Nicolet IS10 spectrometer using a KBr pellet (Thermo Scientific, USA). Transmission electron microscopy (TEM) and high-resolution TEM (HRTEM) images were acquired on a JEM-2100 transmission electron microscope (JEOL, Japan). X-ray diffraction (XRD) pattern was performed on a D2 PHASER diffractometer (Bruker, Germany). Hydrodynamic size distribution and Zeta potential were measured on a Nano-ZSE Zetasizer (Malvern, U.K.). Phosphorescence/fluorescence spectra and luminescence decay curves were performed on an F-7000 spectrofluorometer (Hitachi, Japan). Absorption spectra were acquired on a UV 3600 PLUS UV-vis-NIR spectrophotometer (Shimadzu Co., Japan). Cell imaging was collected on the FV3000 confocal laser scanning microscope (Olympus, Japan). Flow cytometry analysis was recorded on a FACS Calibur flow cytometer (BD Biosciences, USA). *In vivo* luminescence imaging was on performed an IVIS Lumina III imaging system (PerkinElmer, USA). MTT assay were acquired on a Synergy H1 microplate reader (BioTek, America). The content of Zn ion in the solution of major organs and tumors tissue was measured on an X series inductively coupled plasma mass spectrometer (ICP-MS) (Thermo Elemental, UK). All the calculations were carried out on the Gaussian 09 software package.

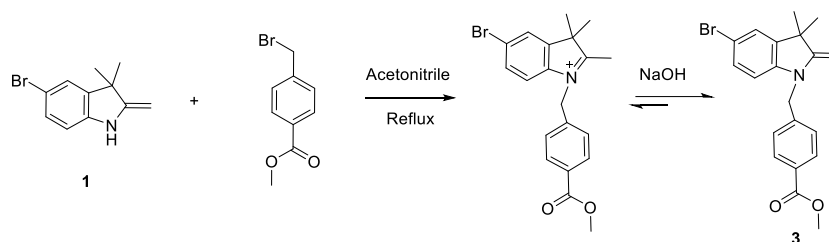
Preparation of photothermal/photodynamic-in-one molecule brominated asymmetric cyanine (BAC)



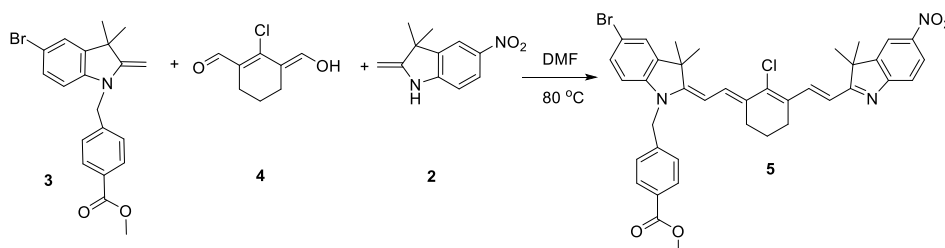
Synthesis of 2,3,3-trimethyl-5-bromo-3H-indoline (compound 1). 4-Bromophenylhydrazine hydrochloride (10 g) was dissolved in high-purity water (150 mL) and then alkalinized to pH 9

with 1 M NaOH solution. The precipitation was collected by filtration, washed twice with high-purity water, followed by vacuum drying overnight to afford 4-bromophenylhydrazine first. Then, 4-bromophenylhydrazine (5.61 g, 30.00 mmol) and methyl isopropyl ketone (3.13 g, 3.90 mL, 36.34 mmol) were added to a round-bottom flask with vigorous stirring at room temperature. After stirring for 1 h, the resulting mixture was extracted with CH₂Cl₂ (50 mL × 3) and concentrated with vacuum rotatory evaporator. Then 30 mL of acetic acid was added and continuously stirred overnight under reflux condition. After cooled to *ca.* 50 °C, partial solvent was evaporated in vacuum, and the resulting solution was diluted with CH₂Cl₂ (100 mL), washed with saturated aqueous K₂CO₃ (50 mL × 4) and high-purity water (50 mL × 2) to neutral, then concentrated to give a red oil. The crude product was purified by silica gel column chromatography with gradient elution (petroleum ether (PE)/ethyl acetate (EA) of 25:1 to 10:1) to give the compound 1 (yellow oil) Yield: 6.41 g, 81%. ¹H NMR (400 MHz, DMSO-d₆, δ): 7.68 (d, *J*= 1.6 Hz, 1H), 7.45 (dd, *J*₁= 8.4 Hz, *J*₂= 2.0 Hz, 1H), 7.37 (d, *J*= 8.0 Hz, 1H), 2.20 (s, 3H), 1.26 (s, 6H); ¹³C NMR (100 MHz, DMSO-d₆, δ): 189.17, 153.21, 149.03, 130.66, 125.49, 121.50, 118.30, 54.34, 22.68, 15.52; MS (ESI+), *m/z*: [M+H]⁺ calcd 238.02, found 238.10.

Synthesis of 2,3,3-trimethyl-5-nitro-3H-indoline (compound 2). The synthetic process is similar to that of compound 1, by using 4-nitrophenylhydrazine (4.59 g, 30.00 mmol) and methyl isopropyl ketone (3.13 g, 3.90 mL, 36.34 mmol). The resulting crude product was purified by silica gel column chromatography with gradient elution (PE/EA of 30:1 to 10:1) to give the compound 2 (yellow powder). Yield: 4.82 g, 78%. ¹H NMR (400 MHz, CDCl₃, δ): 8.28 (dd, *J*₁= 8.4 Hz, *J*₂= 2.0 Hz, 1H), 8.18 (d, *J*= 2.0 Hz, 1H), 7.64 (d, *J*= 8.0 Hz, 1H), 2.28 (s, 3H), 1.40 (s, 6H); ¹³C NMR (100 MHz, CDCl₃, δ): 194.16, 158.95, 146.71, 145.66, 124.53, 120.04, 117.15, 54.50, 22.72, 15.95.

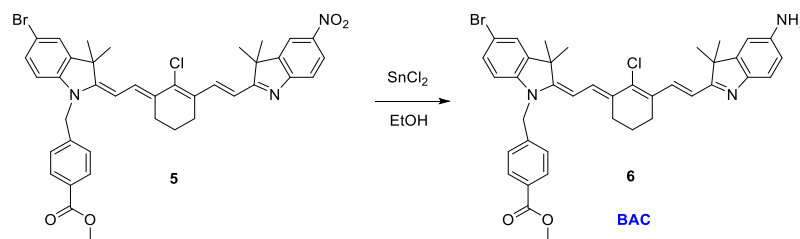


Synthesis of compound 3. 3.57 g (15.00 mmol) of compound 1 and 4.47 g (19.50 mmol) of 4-(bromomethyl) benzoic acid methyl ester were dispersed into 10 mL of CH₃CN, then the resulting mixture was vigorously stirred overnight under reflux condition. After cooled to room temperature, the solvent was evaporated in vacuum, then the resulting red viscous liquids was dissolved in 1 M NaOH (30 mL) and stirred for 2 h at room temperature. The resulting mixture was extracted with CH₂Cl₂ (50 mL × 3) and the combined organic phases were concentrated to afford a red oil. The crude product was purified by silica gel column chromatography with gradient elution (PE/ EA of 60:1 to 30:1) to obtain the title compound as a red oil. Yield: 3.45 g, 59%. ¹H NMR (400 MHz, CDCl₃, δ): 7.99 (d, *J* = 8.4 Hz, 2H), 7.28 (d, *J* = 8.4 Hz, 2H), 7.24 (d, *J* = 2.0 Hz, 1H), 7.19 (dd, *J*₁ = 8.4 Hz, *J*₂ = 2.0 Hz, 1H), 3.92 (s, 3H), 3.89 (s, 2H), 1.41 (s, 6H); ¹³C NMR (400 MHz, CDCl₃, δ): 166.49, 160.73, 144.86, 142.28, 139.74, 130.40, 130.10, 129.28, 126.49, 125.39, 111.17, 106.79, 75.85, 51.97, 45.90, 44.42, 30.07; MS (ESI +), *m/z*: [M+H]⁺ calcd: 386.0750, found 386.00.



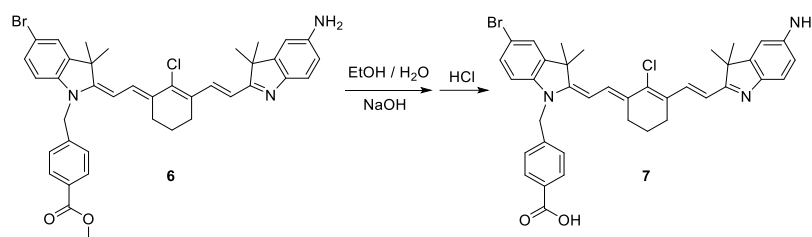
Synthesis of compound 5. 2-chloro-1-formyl-3-(hydroxymethylene)-cyclohex-1-ene (compound 4) was synthesized according to our previously reported method first.¹ Then, to a DMF solution (20 mL) of compound 4 (1.52 g, 8.80 mmol), Compound 2 (1.63 g, 8.00 mmol) and compound 3 (3.09 g, 8.00 mmol) were added, the resulting mixture was then stirred at

80 °C under N₂ atmosphere for 6 h to yield a dark purple solution. After cooled to room temperature, the mixture was poured into frozen diethyl ether (100 mL) and kept at 4 °C for 1 h. After that, the title compound (compound 5) as a purple powder (yield: 3,14 g, 43%) was obtained by filtration, washing with PE, and further purification by silica gel column chromatography with gradient elution (PE/ EA of 20:1 to 3:1). ¹H NMR (400 MHz, CDCl₃, δ): 8.03 (d, *J* = 8.0 Hz, 3H), 7.43 (d, *J* = 8.0 Hz, 2H), 7.31-7.30 (m, 2H), 7.25 (dd, *J*₁ = 8.0 Hz, *J*₂ = 1.6 Hz, 1H), 6.69-6.45 (m, 3H), 6.45 (d, *J* = 8.4 Hz, 1H), 5.44 (d, *J* = 12.8 Hz, 1H), 3.93 (s, 3H), 2.54 (d, *J* = 6.4 Hz, 2H), 2.38 (d, *J* = 6.4 Hz, 2H), 2.24 (s, 1H), 2.07 (s, 1H), 1.82-1.76 (m, 2H), 1.72 (s, 6H), 1.48 (s, 6H); MS (ESI+), *m/z*: [M+H]⁺ calcd 726.17, found 726.20.

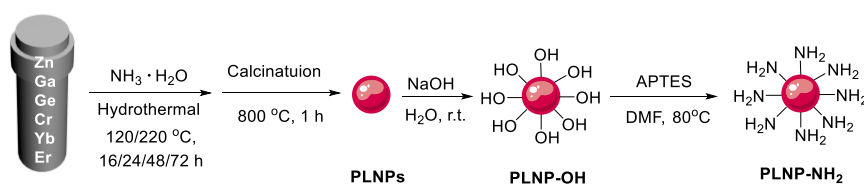


Synthesis of BAC (compound 6). This compound was synthesized according to our previously reported method with slight modifications¹. Briefly, 1.00 g of compound 5 and 2.00 g of tin(II) chloride dihydrate were dispersed into 30 mL of EtOH, and then the resulting mixture was stirred overnight under room temperature. After that, the reaction mixture was poured into 2 M NaOH solution (200 mL), followed by extracting with CH₂Cl₂ (30 mL × 6). The combined organic phases were concentrated to afford a red solid. The crude product was further purified by silica gel column chromatography with gradient elution (PE/ EA of 20:1 to 3:1 to 1:1) to obtain BAC (compound 6) as a red solid. Yield: 0.76 g, 79%. ¹H NMR (400 MHz, CDCl₃, δ): 8.02 (d, *J* = 8.4 Hz, 2H), 7.95 (d, *J* = 16.4 Hz, 1H), 7.43 (d, *J* = 4.8 Hz, 1H), 7.40 (s, 1H), 7.31 (d, *J* = 2.0 Hz, 1H), 7.30 (s, 1H), 7.28 (s, 1H), 7.25 (dd, *J*₁ = 8.4 Hz, *J*₂ = 2.0 Hz, 1H), 7.66 (s, 2H), 6.60 (d, *J* = 6.0 Hz, 1H), 6.45 (d, *J* = 8.0 Hz, 1H), 5.43 (d, *J* = 12.8 Hz, 1H), 4.87 (s, 2H), 3.93 (s, 3H), 2.54 (d, *J* = 6.0 Hz, 2H), 2.37 (d, *J* = 6.0 Hz, 2H), 2.07 (s, 2H), 1.80-1.77 (m, 2H), 1.72 (s, 6H),

1.47 (s, 6H); MS (ESI+), m/z: [M+H]⁺ calcd 696.19, found 696.20.



Synthesis of hydrolyzate of BAC (compound 7). To an ethanol solution (20 mL) of compound 6 (5.54 g, 10 mmol), 2 mL of saturated NaOH solution was added, and then resulting mixture was stirred at 50 °C for 6 h. Whereafter, the solvent was removed, and the resulting residue was re-dissolved in water (20 mL) and acidified to pH = 4-5 with 1 M HCl solution. Finally, the hydrolyzate of BAC was obtained by centrifugation, washing with water and lyophilization with no need for further purification. MS (ESI+), m/z: [M+H]⁺ calcd 682.18, found 682.10.



Preparation of ultra-small size persistent luminescence nanoparticles (PLNPs)

ZGGO:Cr³⁺,Yb³⁺,Er³⁺ persistent luminescence nanoparticles (PLNPs) were synthesized by a surfactant-aided hydrothermal method combined with calcination in air procedure. The hydrothermal and calcination conditions were carefully optimized. Doping elements and doping ratio are in consistent with the stoichiometry of chemical formula (Zn_{1.25}Ga_{1.5}Ge_{0.25}O₄:0.5%Cr³⁺,2.5%Yb³⁺,0.25%Er³⁺) in our previous work.² The detailed synthesis procedures are as follows. 0.74 g of Zn(NO₃)₂ and 16 mg of CTAB were dispersed in 10 mL of high-purity water under vigorous stirring at room temperature, to which 6 mL of Ga³⁺ (0.5 M), 150 μL of Cr³⁺ (0.1 M), 750 μL of Yb³⁺ (0.1 M), 75 μL of Er³⁺ (0.1 M) and 5 mL of Ge⁴⁺ (0.1 M) were added in sequence. The resulting mixture was then adjusted to pH = 8.0 by ammonia solution (30 wt%) and ultrasonicated at room temperature for 0.5 h, and then

vigorously stirred for 1 h. Then the resulting turbid solution was kept at 120 or 220 °C for different time (16 h, 24 h, 48 h or 72 h) via a teflon-lined stainless steel autoclave. After the hydrothermal process, the resulting product was collected by centrifugation (10000 rpm, 10 min), washing sequential with high-purity water (three times) and EtOH (twice), followed by lyophilization. The dried white powder was finally sintered at 800 °C for 1 h or not to acquire ultra-small size PLNPs without further grinding and gradient centrifugation.

For further modifications, the as-prepared PLNPs were further hydroxylated and aminated to obtain hydroxylated PLNPs (PLNP-OH) and amino-functionalized PLNPs (PLNP-NH₂). The detailed hydroxyl/amino functionalized steps are according to our previously reported method.^{2,3} But unlike those, the as-prepared PLNP-OH or PLNP-NH₂ can be directly used in the next step with no need for gradient centrifugation.

Preparation of PLNP-BAC

The BAC-NHS was synthesized first by adding EDC·HCl (0.04 g, 0.21 mmol) and NHS (0.02 g, 0.17 mmol) into a *N,N*-dimethylformamide (DMF) (100 mL) solution of hydrolysate of BAC (0.10 g, 0.15 mmol), and then the resulting mixture was stirred overnight at room temperature in the dark. After that, PLNP-NH₂ (100 mg) and *N,N*-diisopropylethylamine (DIPEA) (0.03 g, 43 μL, 0.25 mmol) were then dispersed to the above solution. The resulting mixture was ultrasonicated for 0.5 h, followed by vigorously stirred for an additional 12 h. Then PLNP-BAC was obtained by centrifugation (10000 rpm, 10 min) and washing sequential with ethanol (EtOH) and high-purity water, followed by lyophilization.

Preparation of PLNP-BAC-PEGBT

The mixture of PLNP-BAC (80 mg) and K₂CO₃ (0.06 g, 0.45 mmol) was dispersed to a chilled DMF solution (80 mL) and ultrasonicated for 0.5 h. Chloroacetyl chloride (22

μL , 0.30 mmol) was then dropwise added to the solution under vigorous stirring at room temperature in the dark. After stirring for 12 h, the resulting mixture was centrifuged (10000 rpm, 10 min), washed with high-purity water for three times and then lyophilized to obtain PLNP-BAC-Cl, which was used in the next reaction without further purification.

The as-prepared PLNP-BAC-Cl was re-dispersed in DMF (60 mL) and ultrasonicated for 0.5 h, then K_2CO_3 (0.03 g) and PEGBT (0.03 g) was added in sequence under vigorous stirring overnight at room temperature in the dark. After that, the resulting PLNP-BAC-PEGBT was collected by centrifugation (10000 rpm, 10 min), washing with high-purity water and EtOH for three times and then lyophilization.

Quantitative analysis of the bond density of BAC on the surface of PLNPs-NH₂

The amount of BAC chemical bonding on the surface of PLNPs-NH₂ was determined with a standard calibration method. Briefly, to measure the bond density of BAC on the surface of PLNPs-NH₂, all of the supernatant was collected and combined during the centrifugation and washing process, and its absorbance at *ca.* 506 nm was measured by UV-vis-NIR spectroscopy. Then, the concentration of BAC in the supernatant was calculated with a standard calibration method (UV-vis-NIR titration of BAC was carried out first at pH 7.4). Finally, the amount of BAC bonding on the surface of PLNPs-NH₂ was further calculated by subtracting the amount of BAC in the supernatant from that of in the initial reaction mixture.

Photostability of BAC

0.75 mL of the BAC (1×10^{-5} M, pH 7.4 or 6.0) was placed in 1.5 ml of Eppendorf tubes and exposed to 0.6 w cm^{-2} of 808 nm laser irradiation for different times (0 s, 10 s, 20 s, 30 s, 40 s, 50 s, 60 s, 1.5 min, 3 min, 5 min, 7 min, 10 min, respectively). ICG (1×10^{-5} M, pH 7.4) irradiated with the same condition was chosen as control. The UV-vis-NIR absorbance

spectral of each solution were recorded before and after irradiation.

Evaluation of *In Vitro* Photothermal Property

To investigate acid-activated photothermal conversion property of the as-synthesized BAC, 0.75 mL of BAC (ethanol/water, 3/7 v/v; 1×10^{-5} M, pH 6.0) was placed in 1.5 mL Eppendorf tubes, followed by irradiation with an 808 nm laser for 10 min at different power densities (0.2 w cm^{-2} , 0.4 w cm^{-2} , 0.6 w cm^{-2} , and 0.8 w cm^{-2} , respectively). The solution of BAC (ethanol/water, 3/7 v/v; 1×10^{-5} M, pH 7.4) and PBS (0.01 M, pH 7.4) irradiated with 808 nm laser (0.6 w cm^{-2}) was set as negative control. ICG (ethanol/water, 3/7 v/v; 1×10^{-5} M, pH 7.4) irradiated with various power densities of 808 nm laser was chosen as positive control. The temperature changes and thermal images of the above solution were recorded in real time using a FLIR E50 thermal imaging camera. The photothermal conversion efficiency of BAC under 0.6 w cm^{-2} of 808 nm irradiation was calculated according to the previously reported.^{4,5}

To evaluate PLNPs as a built-in light source mediated acid-activated and continuous external irradiation-free photothermal effect of PLNP-BAC-PEGBT, 0.75 mL of PLNP-BAC-PEGBT (1 mg mL^{-1} , pH 6.0) was added into 1.5 mL Eppendorf tubes, followed by continuous or fractionated (repeated cycles for 1 min laser on/1 min laser off) irradiation with 10 min of 808 nm laser at 0.6 w cm^{-2} . The same volume solution of PLNPs (1 mg mL^{-1} , pH 7.4 or 6.0) and PLNP-BAC-PEGBT (1 mg mL^{-1} , pH 7.4) continuously irradiated with 808 nm laser (0.6 w cm^{-2} , 10 min) was chosen as control. Besides, BAC (ethanol/water, 3/7 v/v; 1×10^{-5} M, pH 6.0) irradiated with fractionated irradiation was carried out as control as well. The real time changes of temperature and thermal images of each experimental group were also recorded by a FLIR E50 thermal imaging camera.

Evaluation of *In Vitro* Photodynamic Performance

To evaluate acid-activated $^1\text{O}_2$ generation performance of the BAC, DPBF, a sensitive probe of $^1\text{O}_2$, was chosen as an indicator of $^1\text{O}_2$. Acetonitrile solvent required for this experiment was bubbled with air for 1 h before used. Briefly, the mixture of DPBF (6×10^{-5} M in acetonitrile, 900 μL) and BAC (5×10^{-5} M in ethanol, 100 μL) was added to 1.5 mL Eppendorf tubes, and then the pH value of the mixture solution was adjusted to 6.0 by 1 M HCl. Then, the above solution was exposed to continuous 808 nm laser (0.6 w cm^{-2}) irradiation for different times (0 s, 10 s, 20 s, 30 s, 40 s, 50 s, 60 s, 1.5 min, 3 min, 5 min, 7 min, and 10 min), respectively. After that, the absorbance spectra of each solution was recorded on UV-vis-NIR spectrophotometer. It is worth noting that all processes in these experiments should away from light. The blank and control groups were carried out with the following parallel groups and irradiated under the same conditions: DPBF (5.4×10^{-5} M, 1 mL, pH 7.4), DPBF (5.4×10^{-5} M, 1 mL, pH 6.0), DPBF (6×10^{-5} M, 900 μL) with BAC (5×10^{-5} M, 900 μL , pH 7.4) and DPBF (6×10^{-5} M, 900 μL) with ICG (5×10^{-5} M in ethanol, 100 μL , pH 7.4), respectively.

To evaluate PLNPs as a built-in light source mediated acid-activated and continuous external irradiation-free photodynamic performance of PLNP-BAC-PEGBT, the mixture of DPBF (6×10^{-5} M in acetonitrile, 900 μL) and PLNP-BAC-PEGBT (1 mg mL^{-1} in ethanol, 100 μL) was added to 1.5 mL Eppendorf tubes, and then the pH value of the mixture solution was adjusted to 6.0 or 7.4 by 1 M HCl or 1 M NaOH, respectively. Then, the above solution was exposed to continuous or fractionated (repeated cycles for 1 min laser on/1 min laser off) 808 nm laser (0.6 w cm^{-2}) irradiation for different times (0 s, 10 s, 20 s, 30 s, 40 s, 50 s, 60 s, 1.5 min, 3 min, 5 min, 7 min, and 10 min), respectively. The solution of BAC with BPBF irradiated with fractionated 808 nm laser was chosen as control. The absorbance spectra of each solution was recorded on UV-vis-NIR spectrophotometer.

Cellular experiments

Hela cells and A549 cells were purchased from cell bank of Shanghai, Chinese Academy of Science and cultured in DMEM/high-glucose medium and Roswell park memorial institute (RPMI)-1640 medium, respectively. 3T3 fibroblasts were thawed from the frozen cells in our laboratory and incubated in RPMI-1640 medium.

The cytotoxicity and *in vitro* photothermal and photodynamic therapy (PTT/PDT) efficiency was evaluated with a standard MTT assay. In brief, to evaluate the cytotoxicity of PLNP-BAC-PEGBT towards the Hela, A549 and 3T3 cells, each cells were planted in 96-well cell-culture plates (1×10^4 cells/well) and incubated for 24 h. Then, the medium were discarded, followed by addition of fresh medium contained various concentration of PLNP-BAC-PEGBT (20, 40, 80, 100, 150, 200, 300 and 500 $\mu\text{g mL}^{-1}$). The cells incubated with fresh medium only were served as blank control. After incubation for another 12 h, the old medium in each well was replaced by 100 μL of MTT (5 mg mL^{-1} in corresponding medium), and then incubated for another 4 h. Afterwards, the medium was discarded and rinsed twice with PBS buffer, followed by addition of 100 μL of DMSO to dissolve the formazan crystals. Each experiment group was done in quintuplicate. Finally, the absorbance of each well (at 570 nm) was recorded on a microplate reader. The relative cell viability (%) was then calculated by the following formula: viability (%) = (the average absorbance of test group / the average absorbance of the blank control) $\times 100$.

For PTT/PDT efficiency of PLNP-BAC-PEGBT towards the above cells, 808 nm laser irradiation (0.6 w cm^{-2} , continuous irradiation for 2 min or 10 min, or fractionated irradiation for 10 min) was conducted after the addition of PLNP-BAC-PEGBT. After irradiation, the cells were incubated following the similar procedure mentioned above.

To study the cell internalization of PLNP-BAC-PEGBT, Hela, A549 and 3T3 cells were seeded separately in a 6-well plate (5×10^4 cells/well) and cultured overnight at 37 °C. Then the

culture medium was replaced by fresh medium containing PLNPs ($75 \mu\text{g mL}^{-1}$) or PLNP-BAC-PEGBT ($75 \mu\text{g mL}^{-1}$). As a control to verify the tumor active-targeting effect of PEGBT, the above cells were seeded into another 6-well plate and pre-treated with biotin before incubating with PLNP-BAC-PEGBT ($75 \mu\text{g mL}^{-1}$). After incubated for another 12 h, the medium was removed, and then the cells were washed with PBS three times, followed by fixed with formaldehyde (4%, 1.5 mL) and nuclei staining by DAPI. The fixed cells were through rinsed with PBS. Confocal luminescence images were performed on a FV 3000 laser-scanning confocal microscope with a 60 X oil immersion objective lens. To quantify the cell internalization, the cells incubated with PLNPs or PLNPs-probe-PEG ($75 \mu\text{g mL}^{-1}$) were collected and rinsed thoroughly with PBS. Then the luminescent intensity of 20000 events for each group was measured with a FACS Calibur flow cytometer.

Animal experiments

Athymic female Balb/c nude mice (5-6 weeks) were purchased from Slac Laboratory Animal Co. Ltd. All experiments were performed in strict accordance with Chinese National Standard Laboratory animal-Guideline for ethical review of animal welfare (GB/T 35892-2018) and were approved by the Institutional Animal Care and Use Committee of Jiangnan University (Wuxi, China). Hela tumor-bearing model was established by subcutaneous injection of Hela cell (1×10^7 cells) into the right hind leg of the nude mice. *In vivo* imaging and PTT/PDT therapy were carried out when the tumor reached ca. 6 mm in diameter.

For *in vivo* imaging, Hela tumor-bearing mice were randomly divided into two groups (three mice each group), and intravenously injected with PLNP-BAC or PLNP-BAC-PEGBT (4 mg mL^{-1} , $180 \mu\text{L}$), respectively. PLNP-BAC and PLNP-BAC-PEGBT pre-irradiated with a 254 nm UV light for 10 min before injection NIR luminescence imaging was then conducted on an IVIS imaging system at different time point (2, 4, 6, 8 and 12 h). Before acquiring

luminescence images, the mice was excited with LED light (650 ± 10 nm, 5000 lm) for 2 min. All the experiment mice were anesthetized with isoflurane gas to minimize suffering during the whole process. For further monitoring the biodistribution of the nanoprobe, the experiment mice were euthanized and dissected at the design time point. And then tumor tissue and main organs (heart, liver, spleen, lung, kidney, intestines, and stomach) were taken out for *in vitro* imaging. After that, the content of Zn in the above tumor tissue and main organs was determined by ICP-MS after a simple digestion with aqua regia. Tumor tissue and main organs of Hela tumor-bearing mice without treatment were collected and measured as blank.

For *in vivo* PTT/PDT therapy, Hela tumor-bearing mice were randomly divided into six groups (four mice each group). Experiment group (group A and B): PLNP-BAC-PEGBT with continuous or fractionated 808 nm laser irradiation, respectively. Control group (containing group C, D, E and F): Group C: PLNP-BAC-PEGBT; Group D: PBS with continuous 808 nm laser irradiation; Group E: PBS with continuous 808 nm laser irradiation; Group F: untreated. PLNP-BAC-PEGBT (4 mg mL^{-1} , $180 \text{ }\mu\text{L}$ in PBS) was injected into the mice of group A, B and C via a tail vein, respectively, meanwhile $180 \text{ }\mu\text{L}$ of PBS was intravenously injected into the mice of group D and E. Ten-minute continuous 808 nm laser irradiation (0.6 W cm^{-2}) was carried out to the tumor tissues of group A and group C at 8 hours after injection, and fractionated 808 nm laser irradiation (0.6 W cm^{-2} , repeated cycles for 1 min laser on/1 min laser off) was applied to group B and group E. The temperature increase of tumor tissues was monitored by IR thermal camera. The tumor volume and body weight of each mouse were recorded every two days for 12 days. The tumor volume was calculated as $\text{length} \times \text{width}^2 \times 0.5$, length and width are the greatest longitudinal diameter and the greatest transverse diameter, respectively, which were measured by a vernier caliper. In order to reflect the tumor growth

intuitively, the relative tumor volume for each mouse was calculated as the tumor volume at different time / the original tumor volume before treatment.

To investigate whether fractionated laser irradiation can effectively reduce damage of laser itself compared with the traditional continuous irradiation, high powered fractionated and continuous 808 nm laser irradiation (1.0 W cm⁻² and 1.5 W cm⁻², repeated cycles for 1 min laser on/1 min laser off or laser always on) were applied to the mice without any treatment, respectively. The temperature increase of the irradiated sites were monitored by IR thermal camera. The appearance change were recorded on camera.

To further investigate the *in vivo* therapeutic mechanism and the potential systemic toxicity of the designed PLNP-BAC-PEGBT platform, histological (hematoxylin and eosin staining, H&E staining) and immunohistochemical (IHC) analysis (including Ki67 and cleaved caspase 3 for cells proliferation and apoptosis, respectively) were carried out at 24 h post treatments and after the whole therapeutic process. For this purpose, all the mice were euthanized at a specified time, and then main organs (heart, liver, spleen, lung and kidney) and tumor tissues were collected and fixed with 4% formaldehyde, and then embedded in paraffin and sectioned at 5 μm thickness for H&E staining and IHC analysis.

Supplementary References.

1. X. Zhao, Y. Li, D. Jin, Y. Z. Xing, X. L. Yan, and L. G. Chen. *Chem. Commun.* 2015, **51**, 11721-11724.
2. Y. J. Li, and X. P. Yan. *Nanoscale*, 2016, **8**, 14965-14970.
3. A. Abdukayum, J. T. Chen, Q. Zhao, and X. P. Yan. *J. Am. Chem. Soc.* 2013, **135**, 14125-14133.
4. Y. F. Wang, W. Du, T. Zhang, Y. Zhu, Y. H. Ni, C. C. Wang, F. M. S. Raya, L. W. Zou, L. S. Wang, G. L. Liang. *ACS Nano*, 2020, **14**, 9585-9593.

5. J. Cui, R. Jiang, C. Guo, X. Bai, S. Xu, L. Wang. *J. Am. Chem. Soc.* 2018, **140**, 5890-5894.

Supplementary Figures

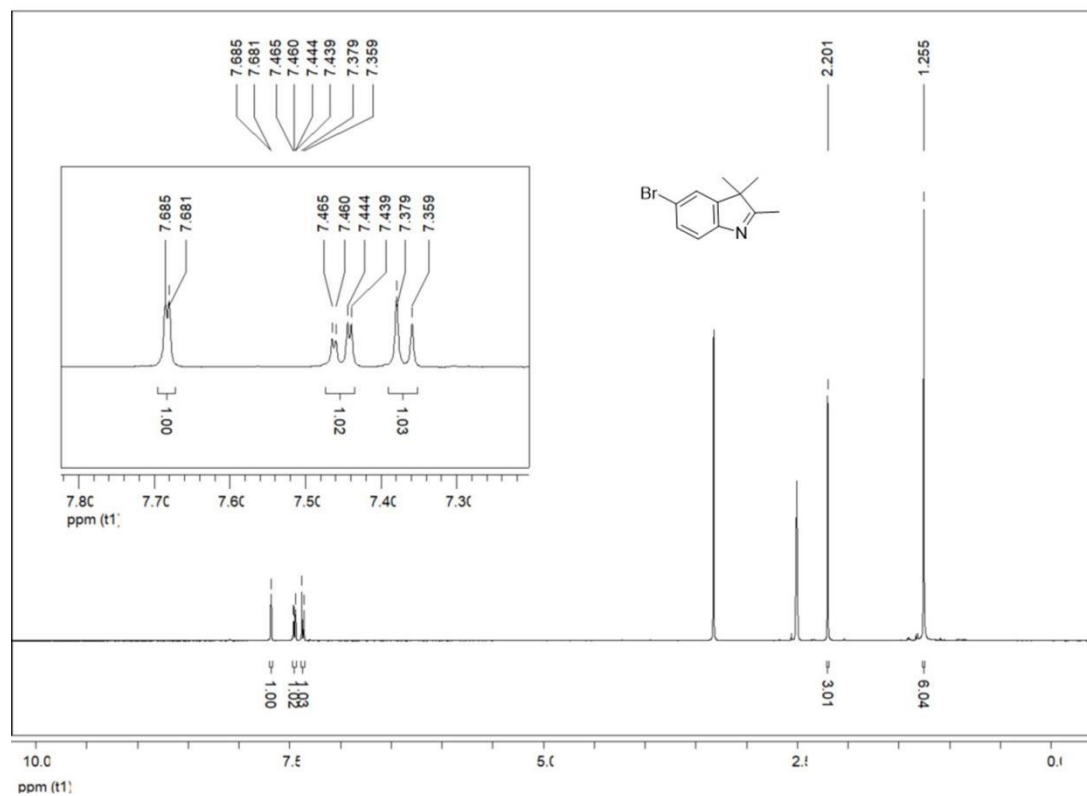


Fig. S1 ^1H NMR spectrum of 2,3,3-trimethyl-5-bromo-3H-indoline (compound 1).

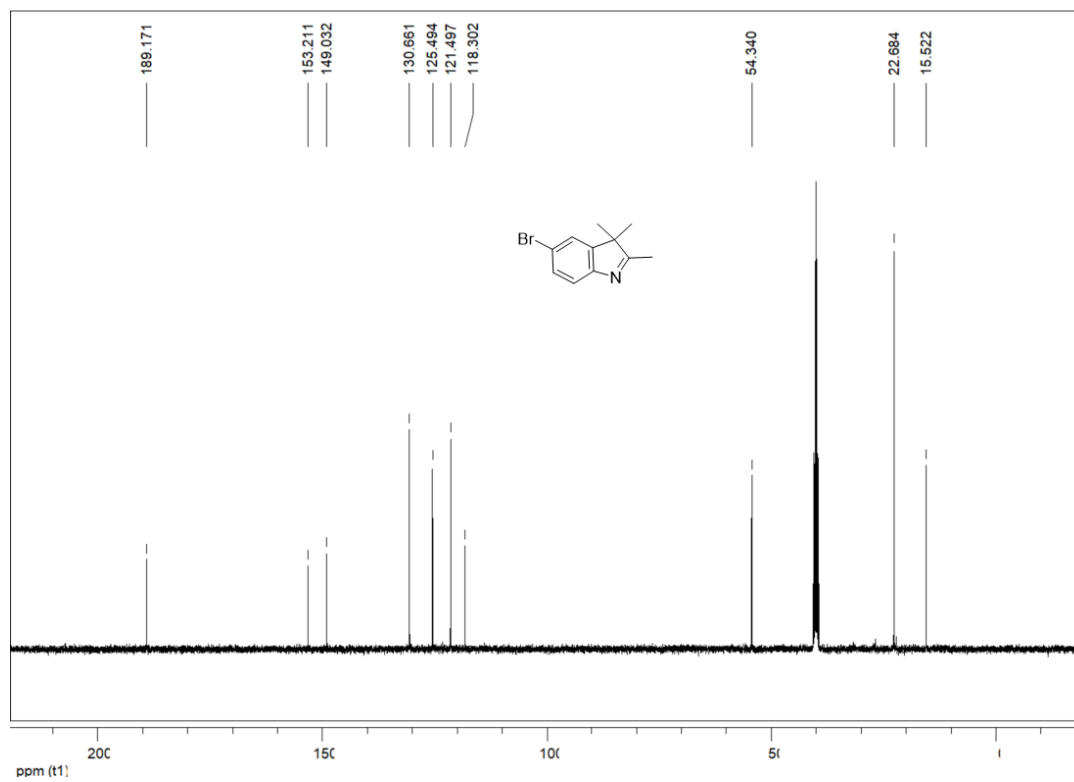


Fig. S2 ^{13}C NMR spectrum of 2,3,3-trimethyl-5-bromo-3H-indoline (compound 1).

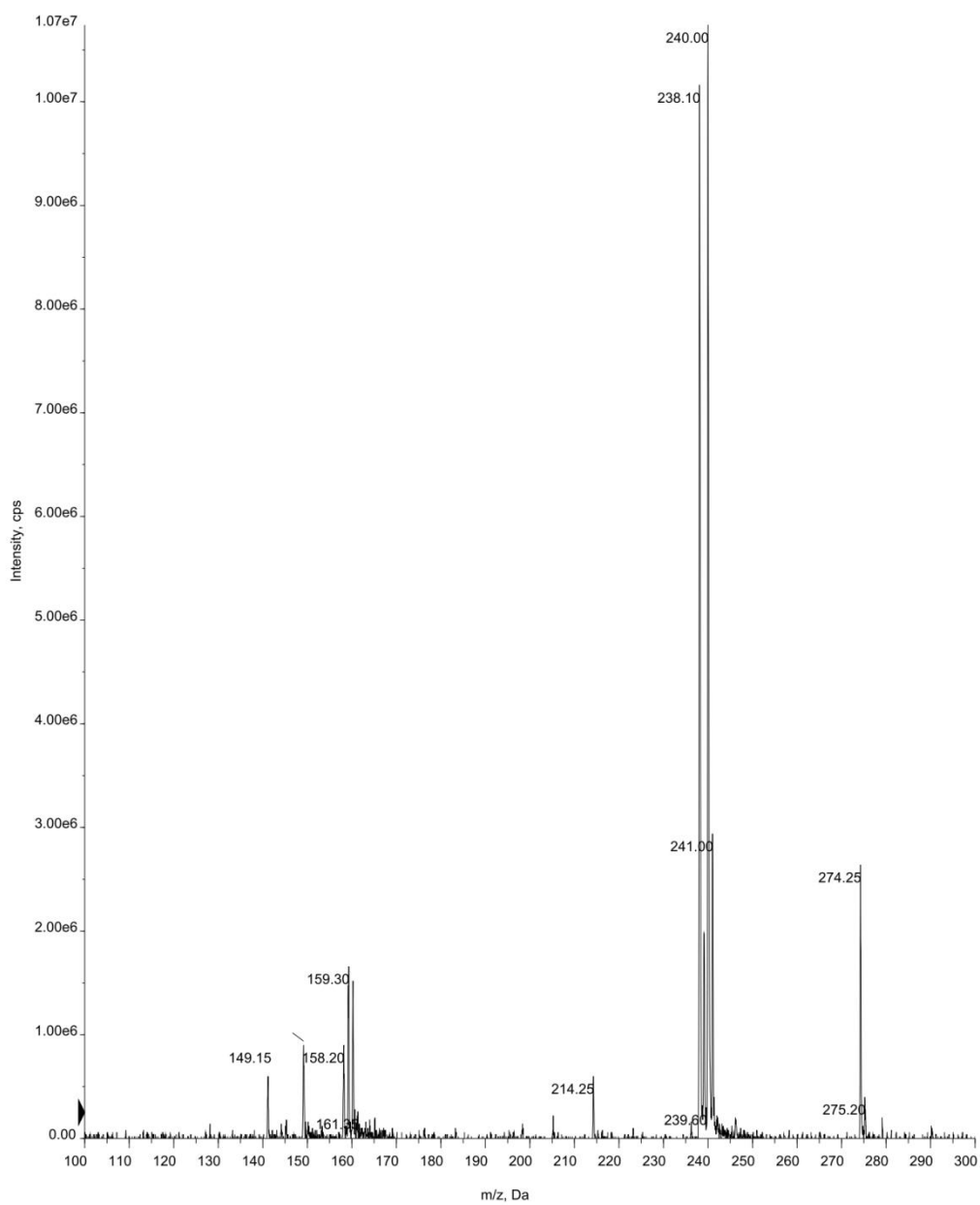


Fig. S3 MS spectrum of 2,3,3-trimethyl-5-bromo-3*H*-indoline (compound 1).

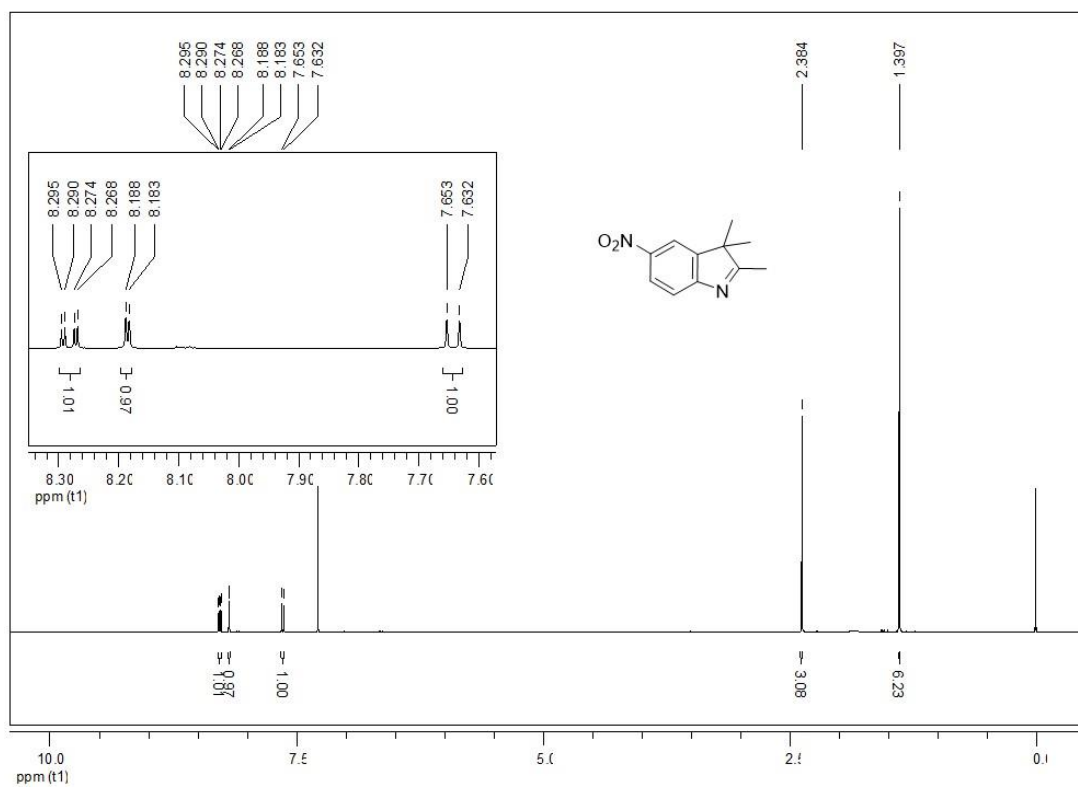


Fig. S4 ¹H NMR spectrum of 2,3,3-trimethyl-5-nitro-3H-indoline (compound 2).

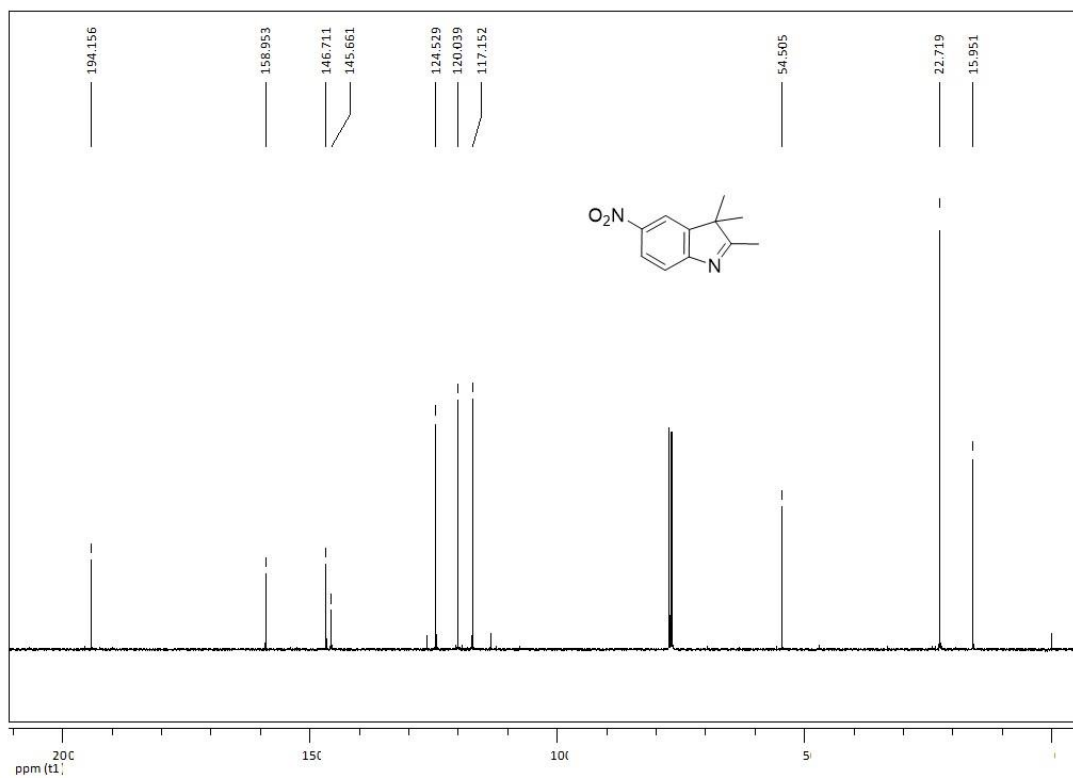


Fig. S5 ¹³C NMR spectrum of 2,3,3-trimethyl-5-nitro-3H-indoline (compound 2).

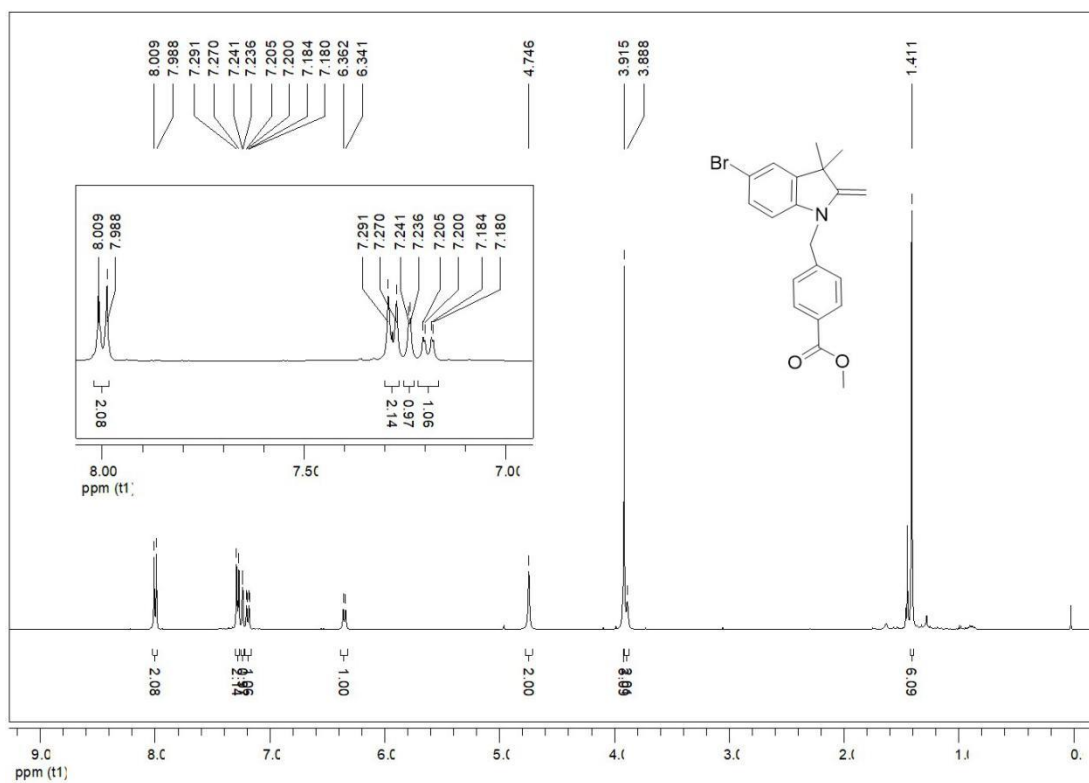


Fig. S6 ¹H NMR spectrum of compound 3.

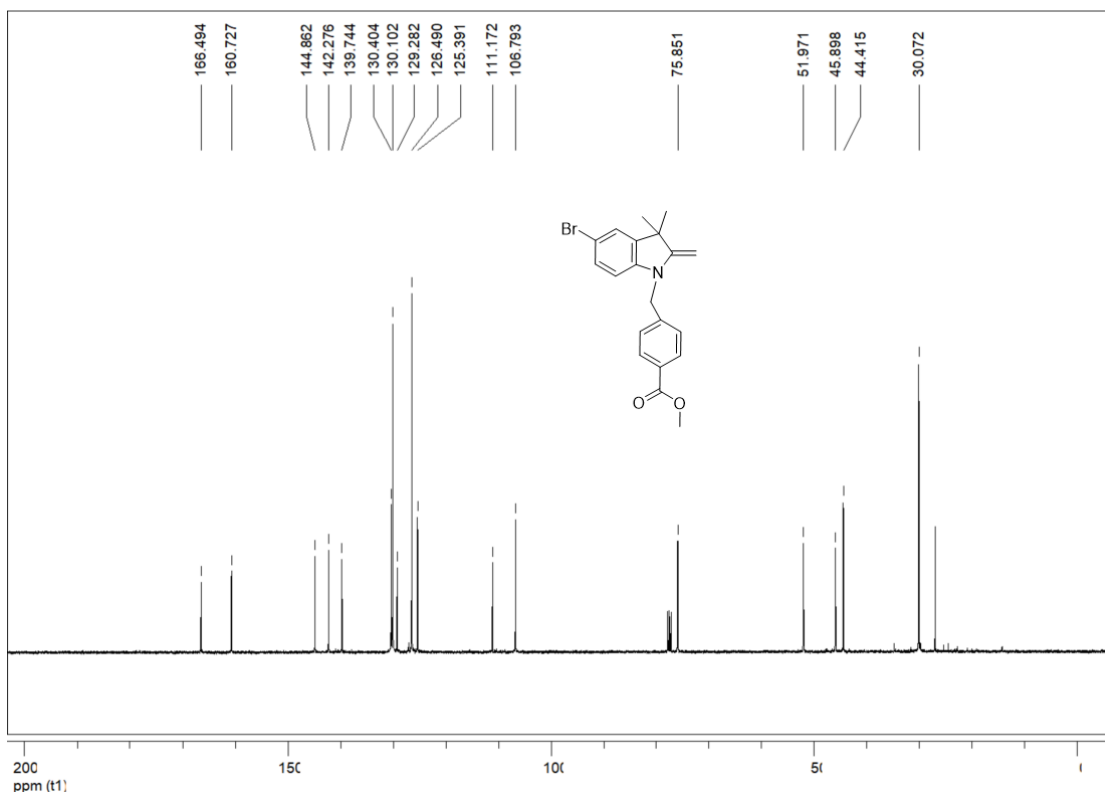


Fig. S7 ¹³C NMR spectrum of compound 3.

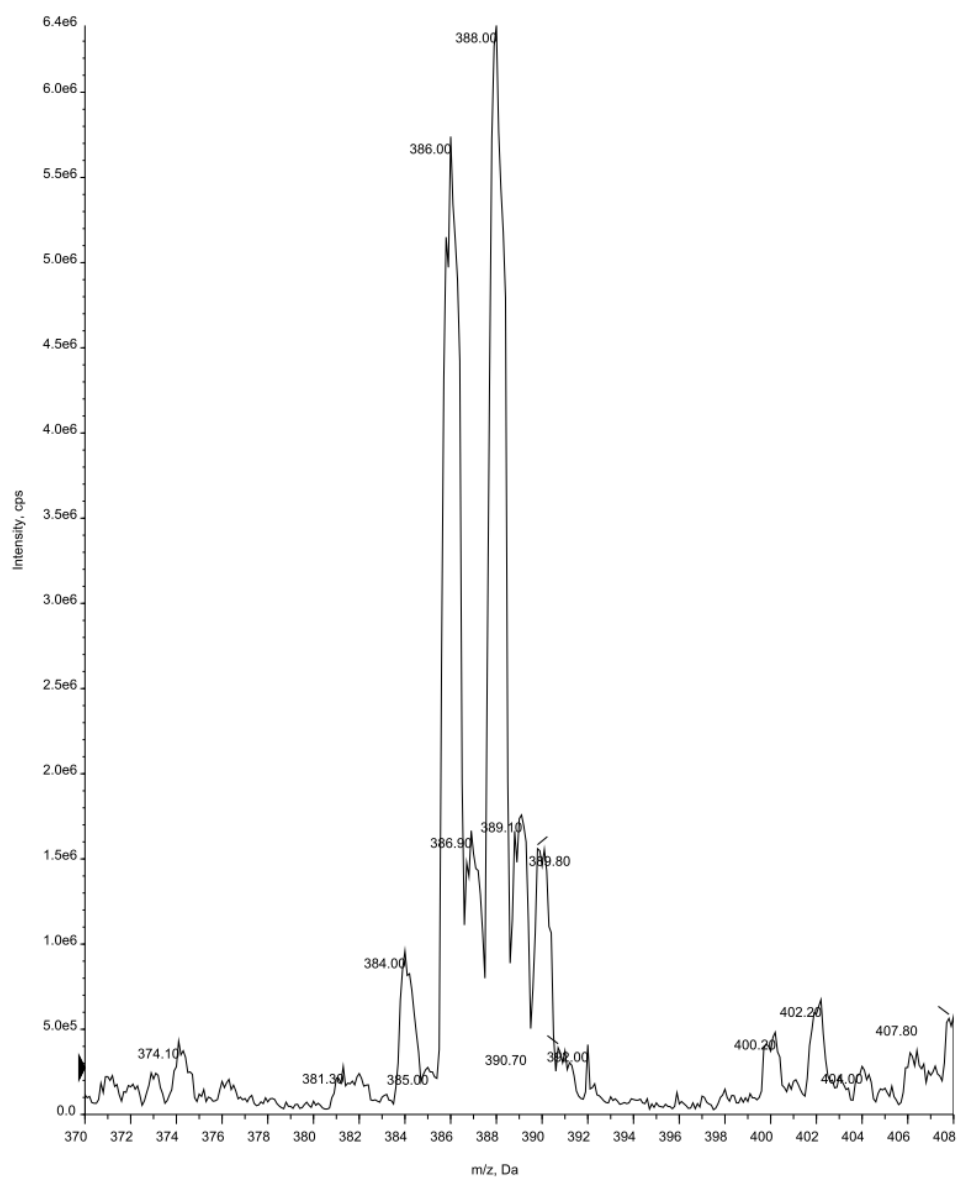


Fig. S8 MS spectrum of compound 3

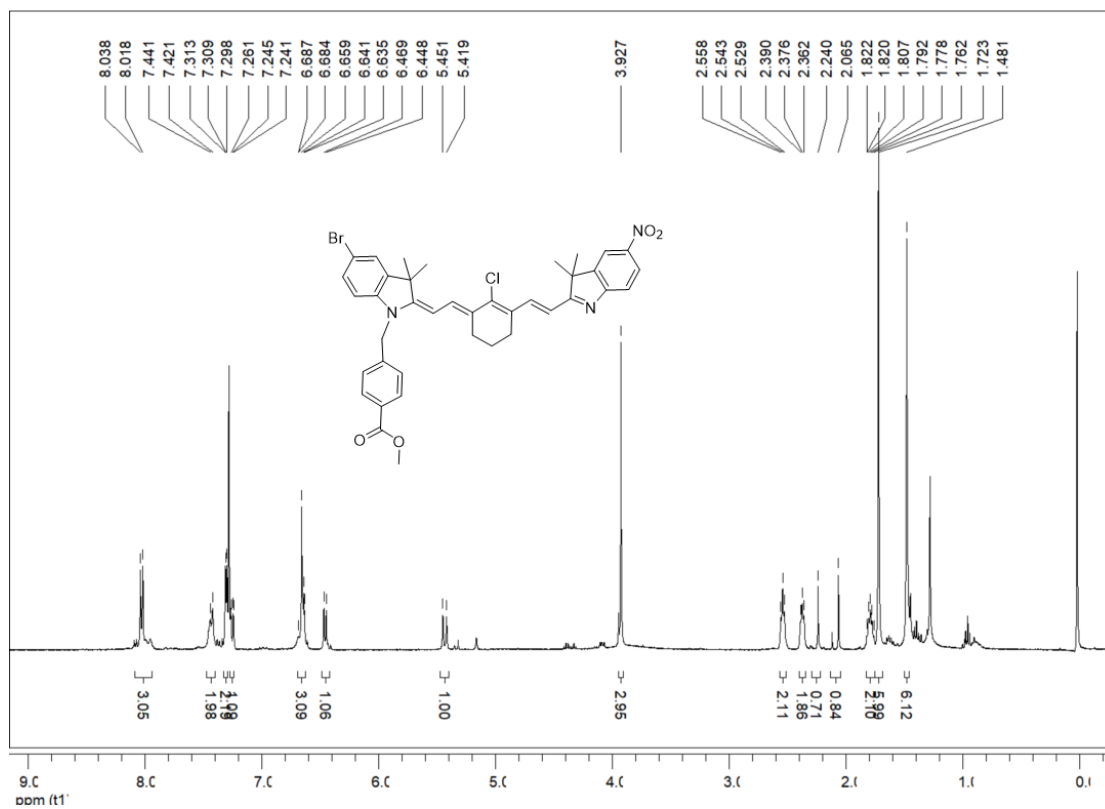


Fig. S9 ¹H NMR spectrum of compound 5.

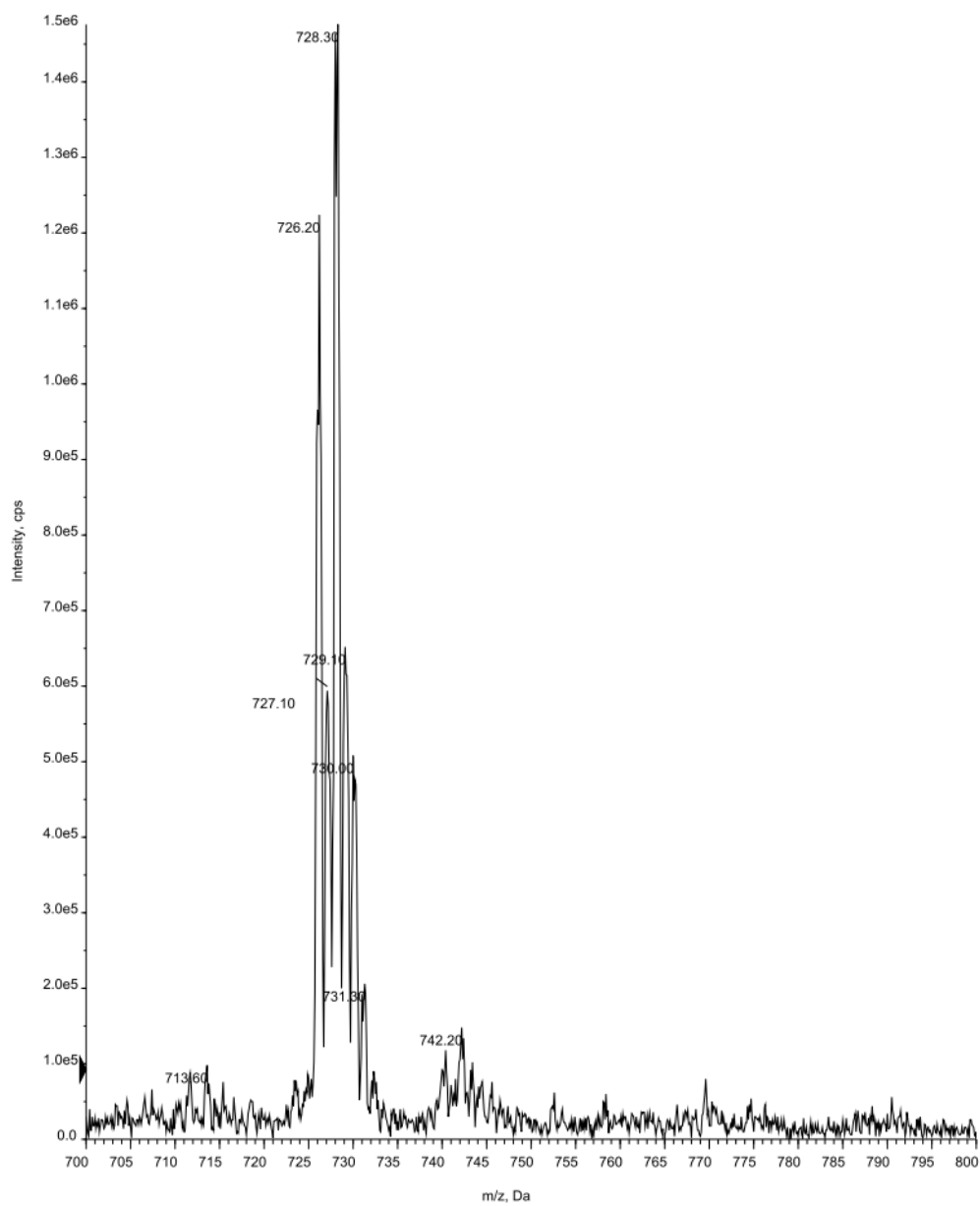


Fig. S10 MS spectrum of compound 5.

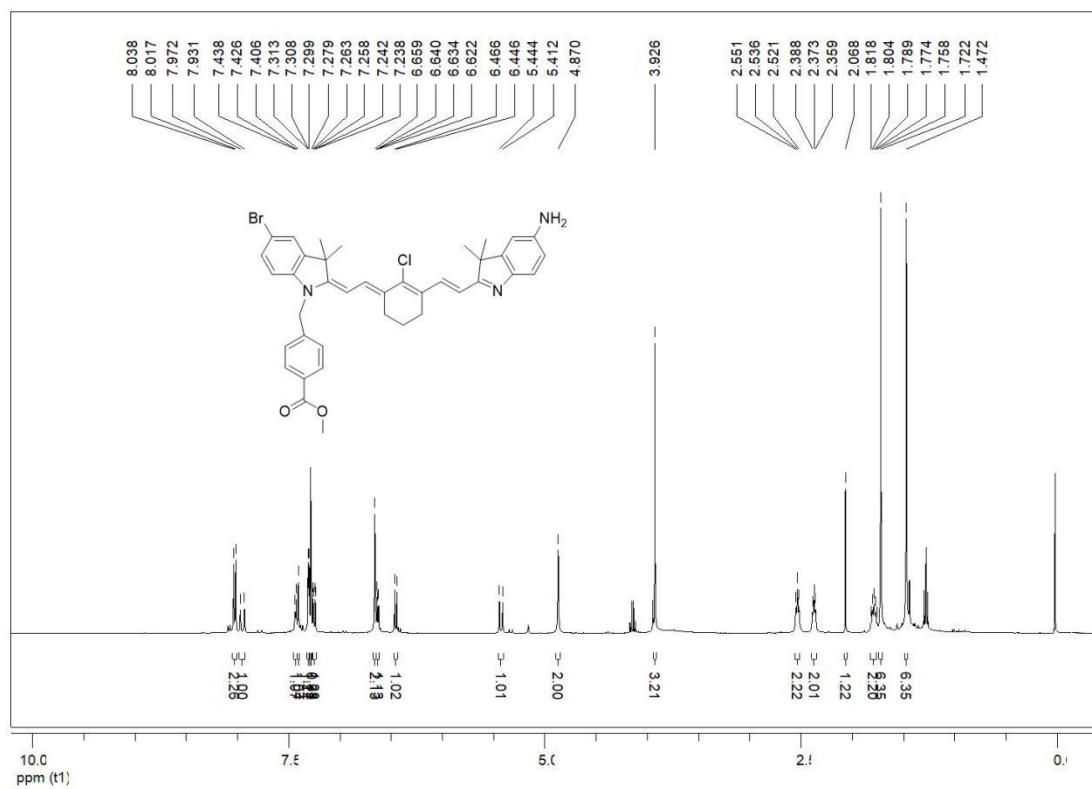


Fig. S11 ¹H NMR spectrum of BAC (compound 6).

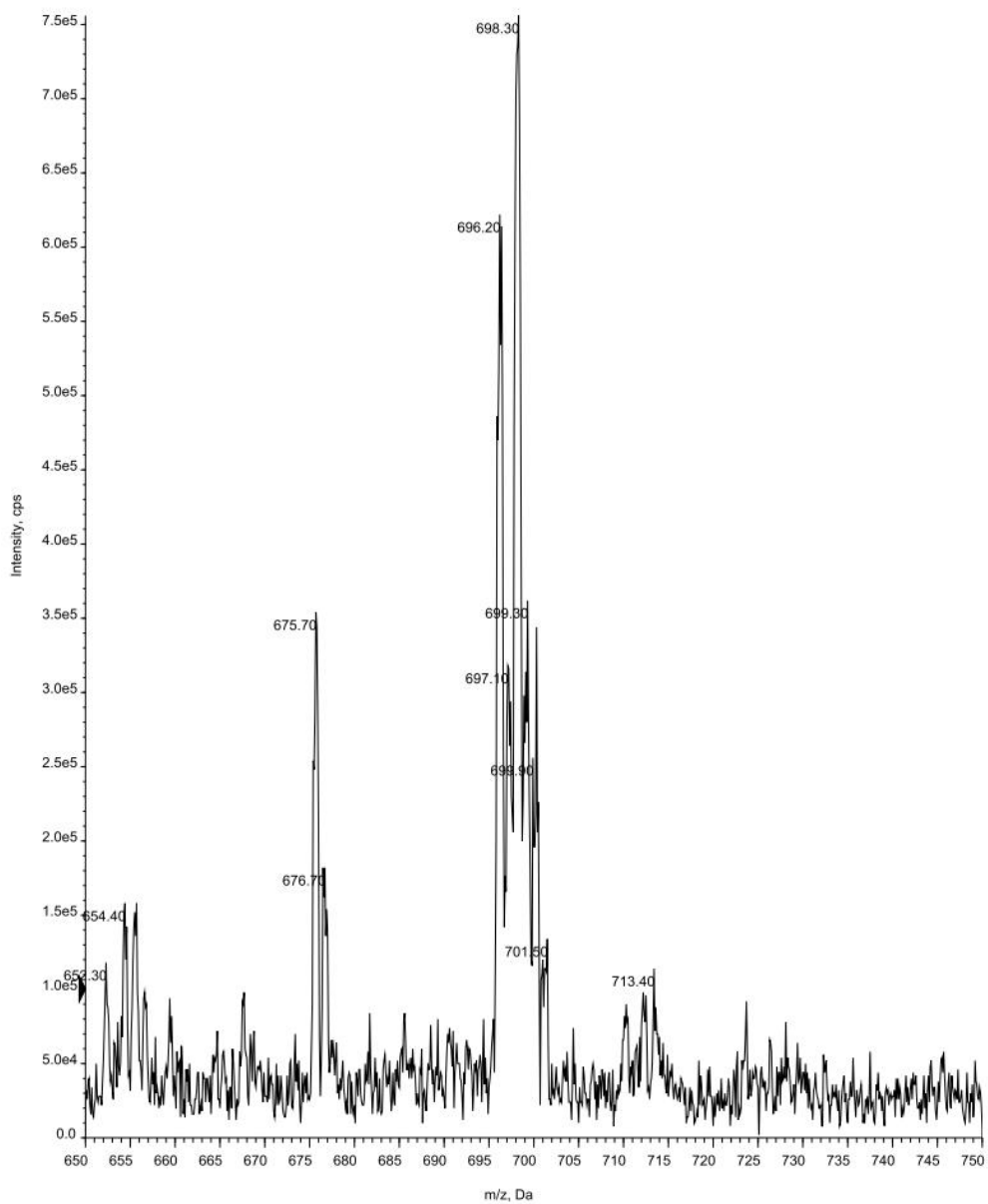


Fig.S12 MS spectrum of BAC (compound 6).

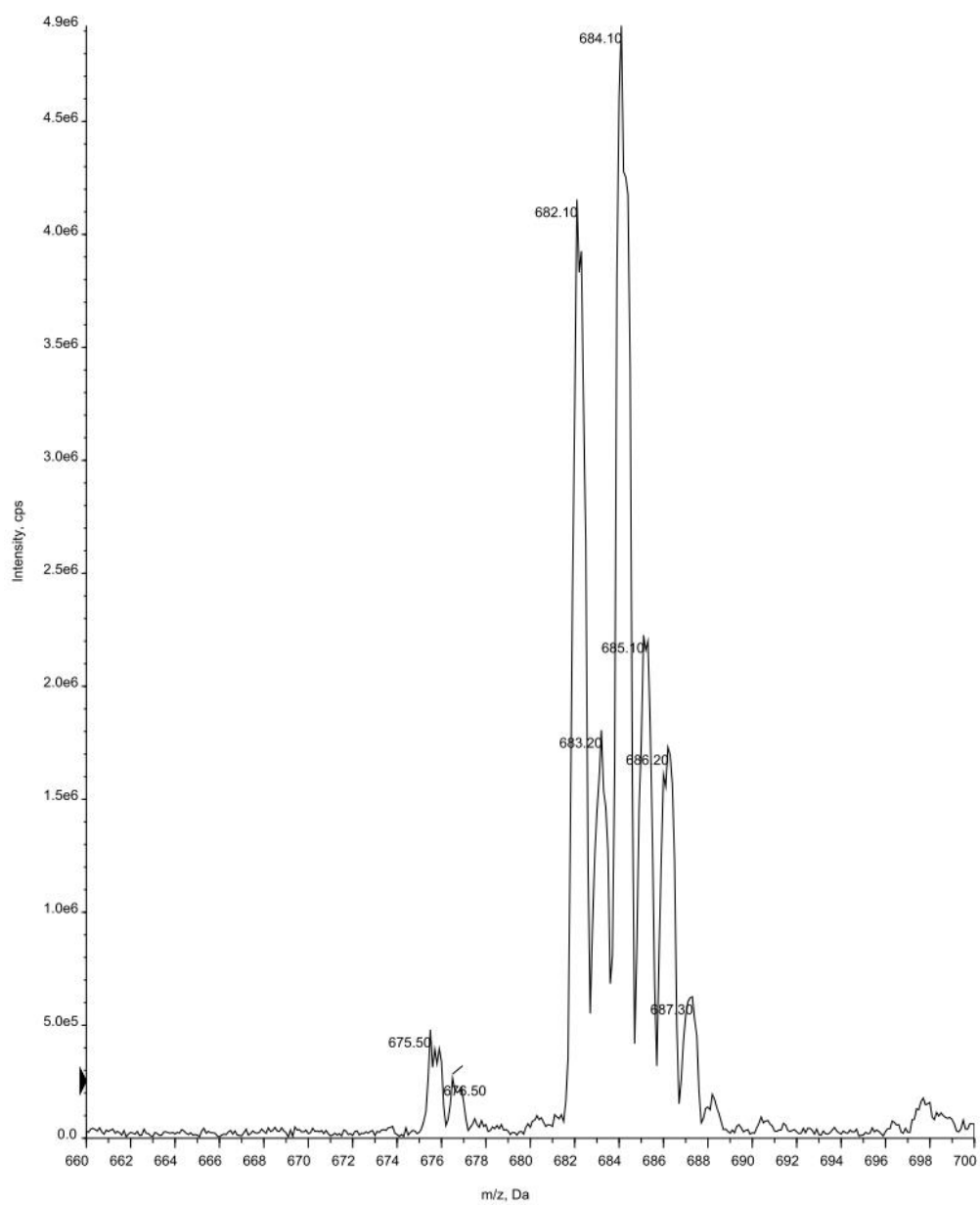


Fig. S13 MS spectrum of the hydrolyzate of BAC (compound 7).

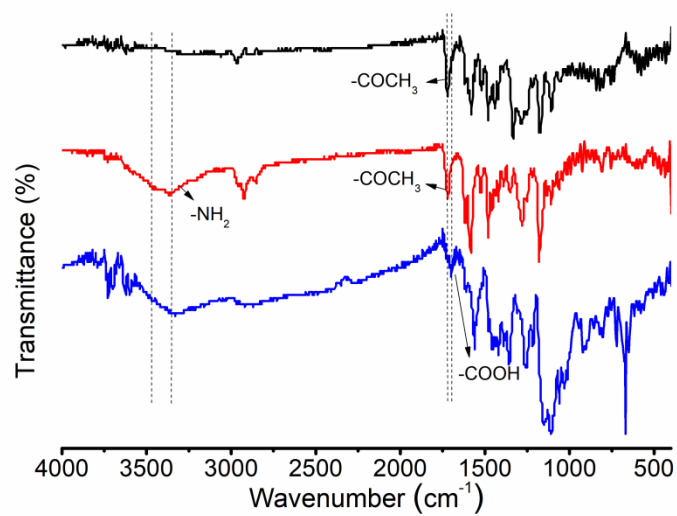


Fig. S14 FT-IR spectra of the compound 5 (black curve), BAC (compound 6, red curve) and the hydrolysate of BAC (compound 7, blue curve).

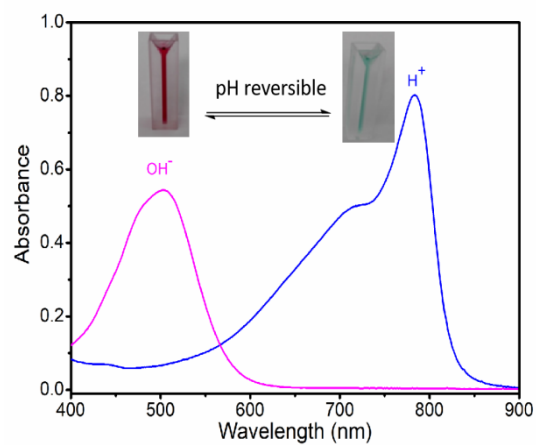


Fig. S15 Reversible characteristic absorption and solution color change of BAC with pH.

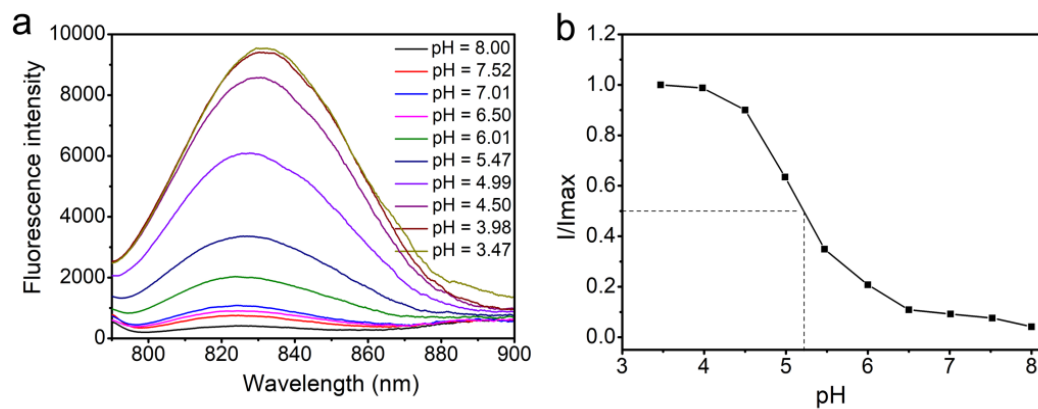


Fig. S16 a Fluorescence spectra of BAC (1×10^{-5} M) at different pH values. **b** pH dependent fluorescence response of BAC as a plot of I/I_{\max} vs. pH. I is the fluorescence intensity of BAC at different pH values. I_{\max} is the fluorescence intensity of BAC at pH 3.47.

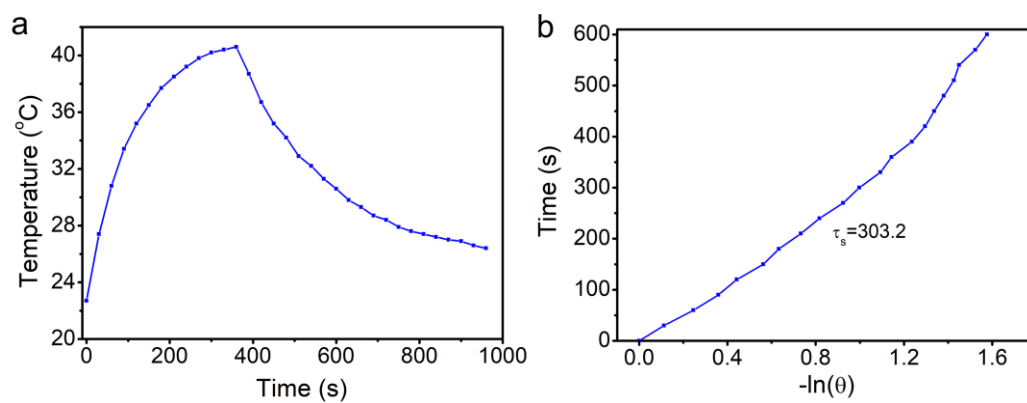


Fig. S17 a Temperature change curve of BAC under 5 minutes of 808 nm laser irradiation (0.6 w cm^{-2}) and 10 minutes of natural cooling. **b** Time constant (τ_s) of this system. $\theta = (T - T_{\text{surr}})/(T_{\text{max}} - T_{\text{surr}})$, T_{max} , T and T_{surr} are the maximum laser-triggered solution temperature, laser-triggered solution temperature at a certain time and the ambient temperature.

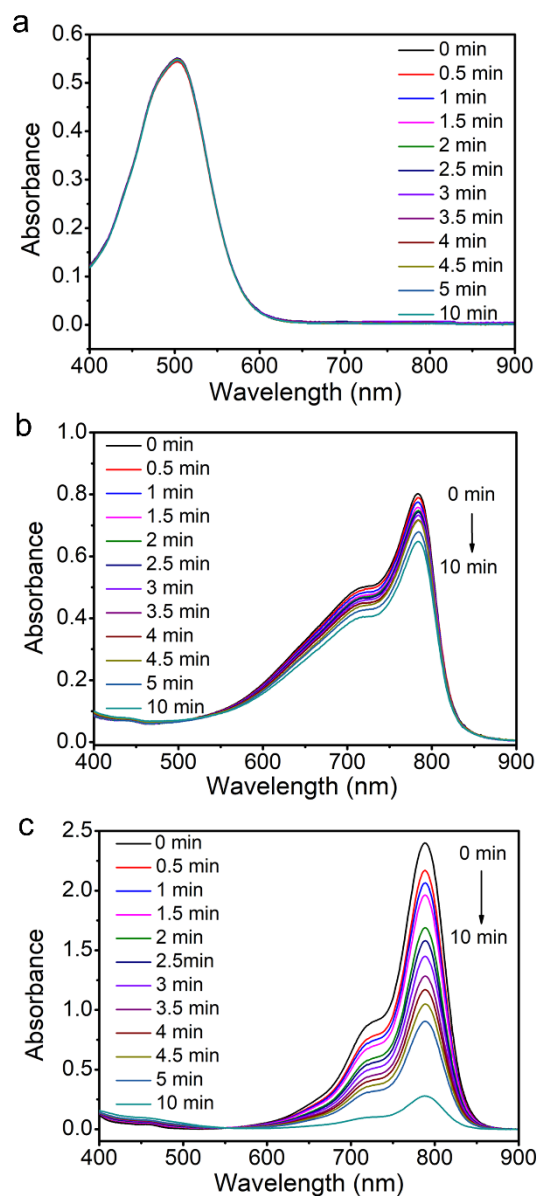


Fig. S18 Stability of BAC and ICG under the irradiation of 808 nm laser (0.6 w cm^{-2}). **a** UV-vis-NIR absorption spectra of BAC at pH 7.4 under 808 nm laser irradiation. **b** UV-vis-NIR absorption spectra of BAC at pH 6.0 under 808 nm laser irradiation. **c** UV-vis-NIR absorption spectra of ICG at pH 7.4 under 808 nm laser irradiation.

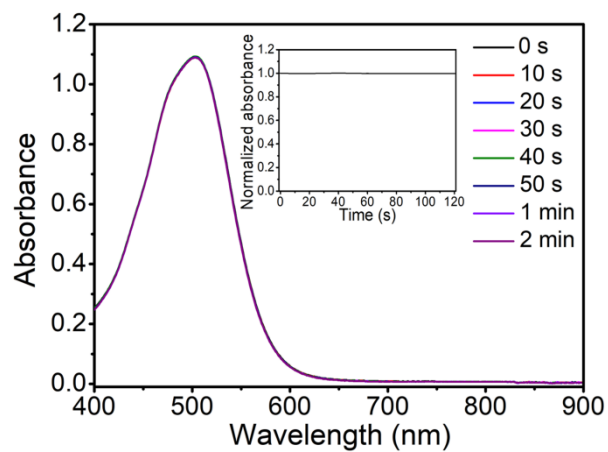


Fig.S19 Stability of BAC under the irradiation of 650 nm LED lamp. UV-vis-NIR absorption spectra of BAC at pH 7.4 under 650 nm LED lamp irradiation. Inset is the plot of the relative absorbance of BAC at pH 7.4 at 506 nm against irradiation time.

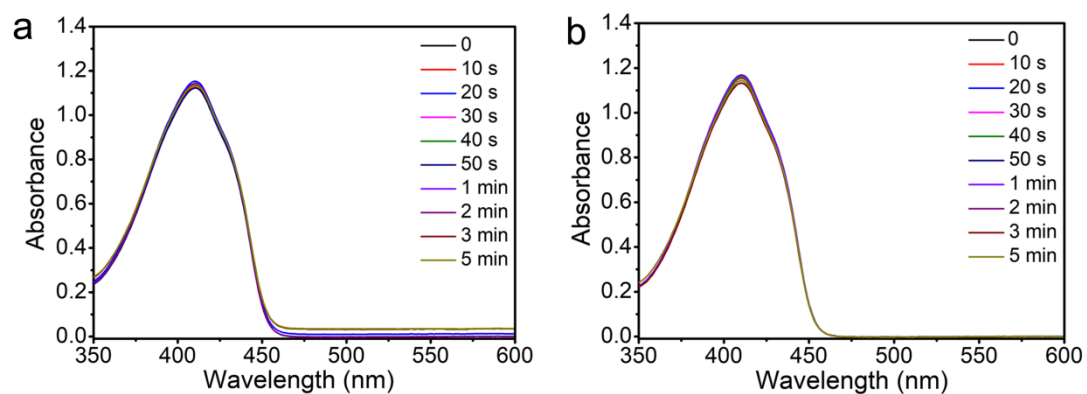


Fig. S20 Stability of DPBF under the irradiation of 808 nm laser (0.6 w cm^{-2}). **a** UV-vis-NIR absorption spectra of DPBF ($5.4 \times 10^{-5} \text{ M}$) at pH 7.4 under 808 nm laser irradiation. **b** UV-vis-NIR absorption spectra of DPBF ($5.4 \times 10^{-5} \text{ M}$) at pH 6.0 under 808 nm laser irradiation.

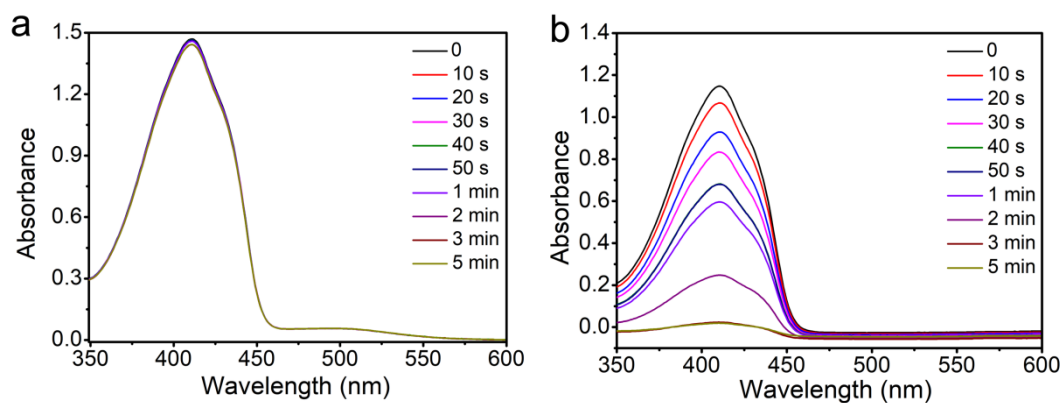


Fig. S21 pH-activated $^1\text{O}_2$ generation ability of BAC under continuous 808 nm laser irradiation (0.6 w cm^{-2}). **a** UV-vis-NIR absorption spectra of DPBF ($5.4 \times 10^{-5} \text{ M}$) in the presence of BAC ($5.0 \times 10^{-6} \text{ M}$) at pH 7.4 under continuous 808 nm laser irradiation. **b** UV-vis-NIR absorption spectra of DPBF ($5.4 \times 10^{-5} \text{ M}$) in the presence of BAC ($5.0 \times 10^{-6} \text{ M}$) at pH 6.0 under continuous 808 nm laser irradiation.

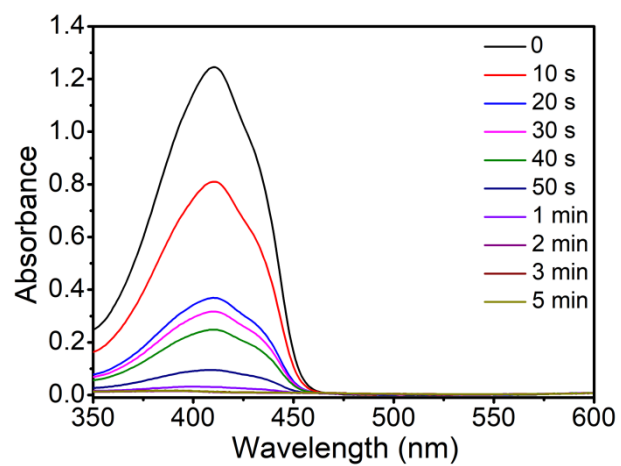


Fig. S22 ¹O₂ generation ability of ICG under continuous 808 nm laser irradiation (0.6 w cm⁻²). UV-vis-NIR absorption spectra of DPBF (5.4 × 10⁻⁵ M) in the presence of ICG (5.0 × 10⁻⁶ M) at pH 7.4 under continuous 808 nm laser irradiation.

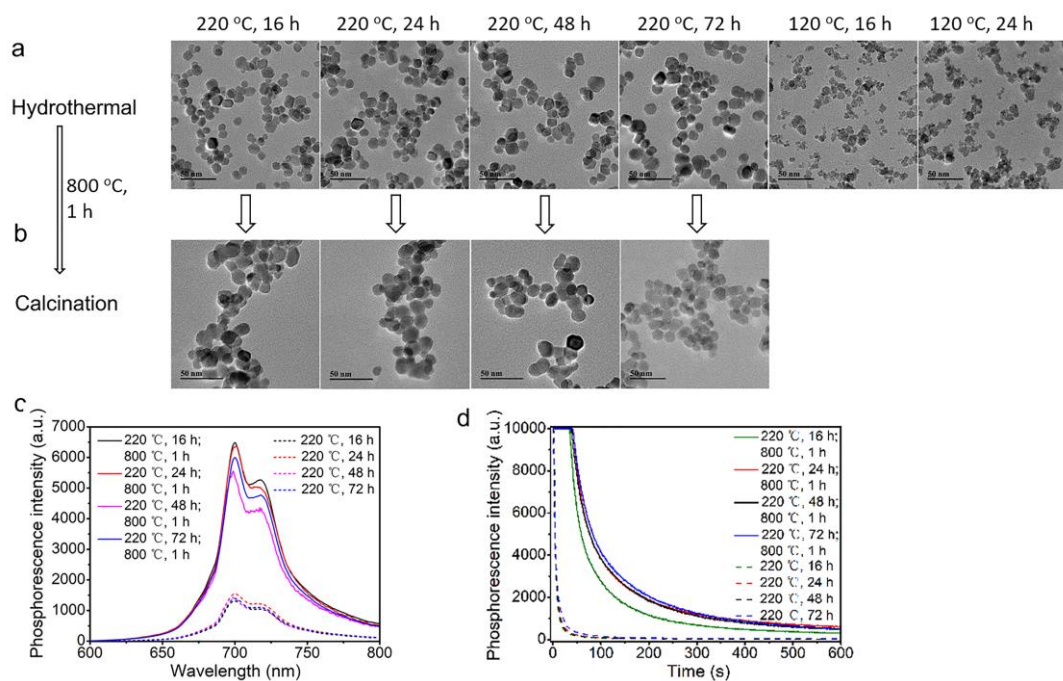


Fig. S23 Characterization of PLNPs prepared under different hydrothermal and calcination conditions. **a** TEM images of PLNPs under different hydrothermal times and temperatures. **b** TEM images of PLNPs under different hydrothermal and calcination conditions. **c** Photoluminescence spectra of PLNPs under different hydrothermal and calcination conditions. **d** Persistent luminescence decay curves of PLNPs under different hydrothermal and calcination conditions, monitored at 695 nm after 10 min irradiation with 254 nm UV lamp.

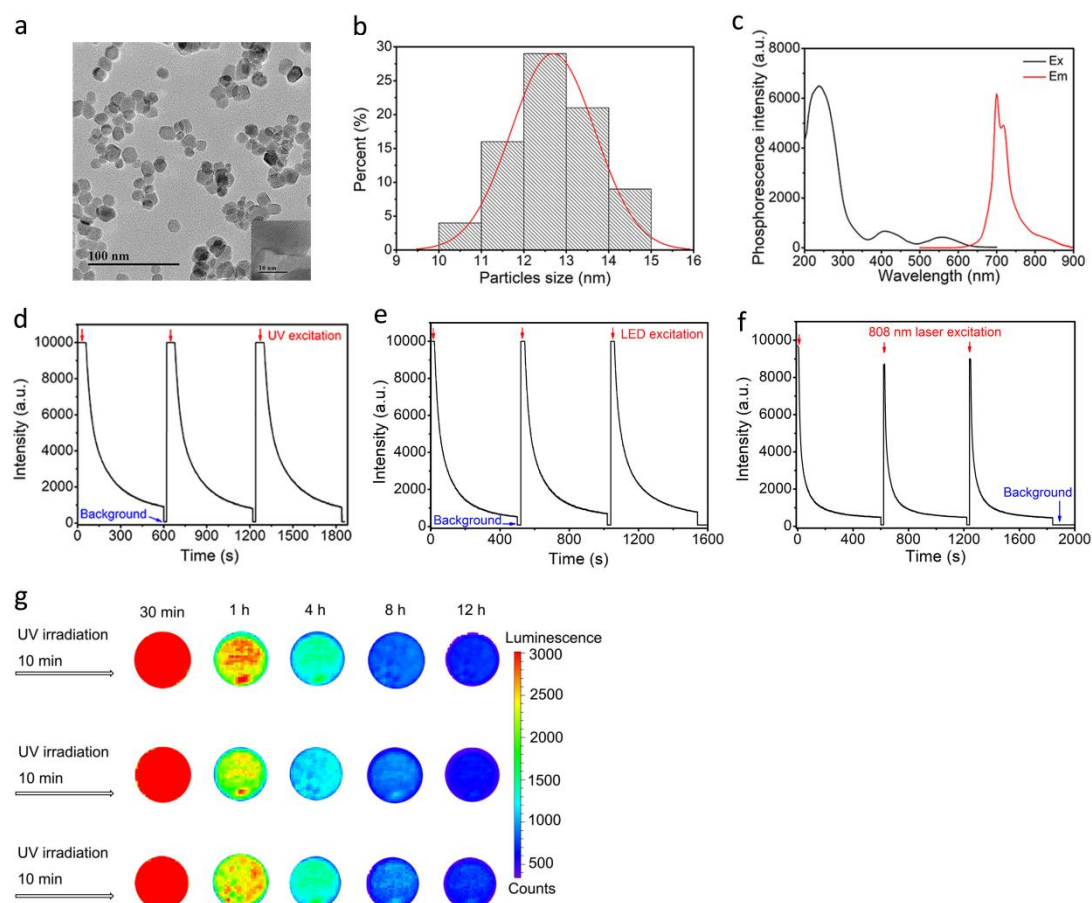


Fig. S24 Characterization of the as-prepared PLNPs. **a** TEM images (Inset is the lattice structure of PLNPs). **b** Size distribution of PLNPs. **c** Excitation (em. 691 nm) and emission (ex. 254 nm) spectra. **d** Persistent luminescence decay curves of PLNPs monitored at 695 nm under the excitation of 10 min of 254 nm UV lamp. The samples were re-activated with 254 nm UV lamp for 10 min before each measurement. **e** Persistent luminescence decay curves of PLNPs monitored at 695 nm under the excitation of 2 min of 650 nm LED lamp. The samples were re-activated with LED lamp for 2 min before each measurement. **f** Persistent luminescence decay curves of PLNPs monitored at 695 nm after 2 min of 808 nm laser irradiation. The samples were re-activated with 808 nm laser for 2 min before each measurement. **g** UV-reactivated persistent luminescence images of PLNPs. The PLNPs was pre-irradiated with a UV lamp for 10 min before luminescence images and the natural decay of persistent luminescence signal was collected by CCD camera without excitation.

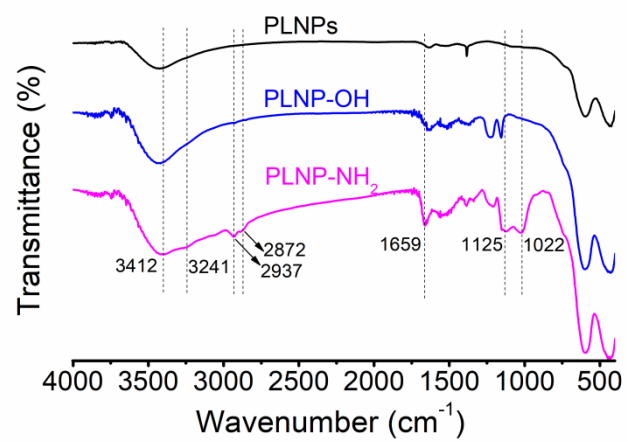


Fig. S25 FT-IR spectra of PLNPs, PLNP-OH and PLNP-NH₂.



Fig. S26 Photographs of PLNPs and PLNP-BAC at pH 7.4.

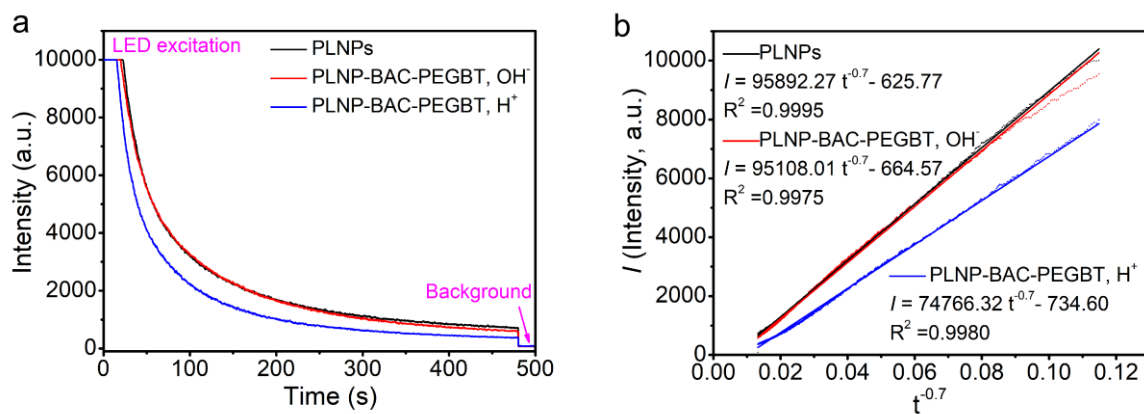


Fig. S27 a Persistent luminescence decay curves of PLNPs and PLNP-BAC-PEGBT at pH 6.0 and 7.4, monitored at 695 nm after 2 min of 650 nm LED lamp irradiation. **b** The plot of persistent luminescence intensity (I) vs. time ($t^{-0.7}$) for PLNPs and PLNP-BAC-PEGBT at pH 6.0 and 7.4, and the linearly relationship of $I(t^{-0.7})$ indicates the persistent luminescence emission of them all through a tunneling or temperature-assisted tunneling process.²

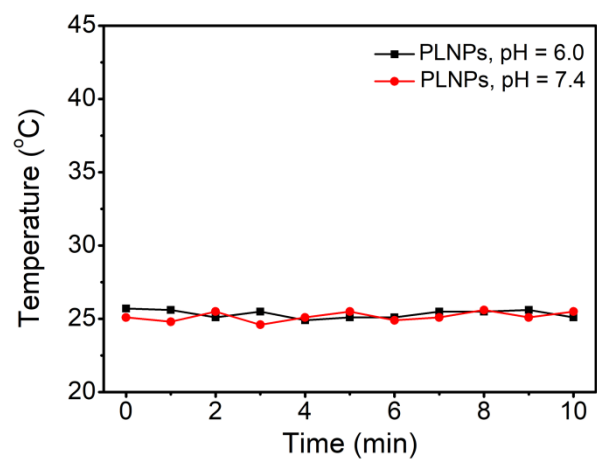


Fig. S28 Temperature change curves of PLNPs at pH 7.4 and 6.0 under the continuous 808 nm laser irradiation (0.6 w cm^{-2}).

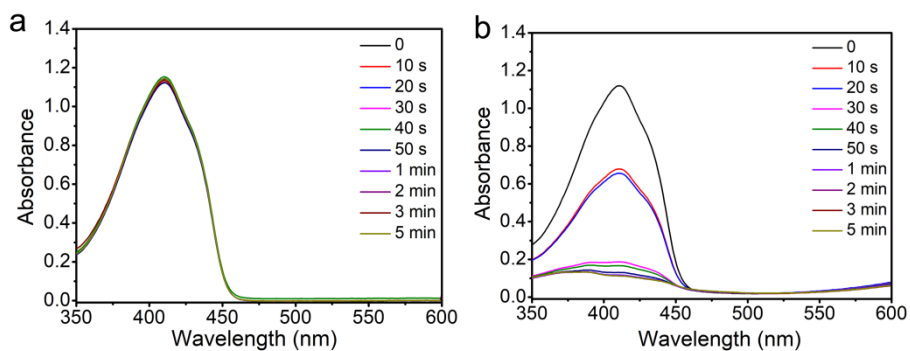


Fig. S29 pH-activated $^1\text{O}_2$ generation ability of PLNP-BAC-PEGBT under continuous 808 nm laser irradiation (0.6 w cm^{-2}). **a** UV-vis-NIR absorption spectra of DPBF ($5.4 \times 10^{-5} \text{ M}$) in the presence of PLNP-BAC-PEGBT (1 mg mL^{-1}) at pH 7.4 under continuous 808 nm laser irradiation. **b** UV-vis-NIR absorption spectra of DPBF ($5.4 \times 10^{-5} \text{ M}$) in the presence of PLNP-BAC-PEGBT (1 mg mL^{-1}) at pH 6.0 under continuous 808 nm laser irradiation.

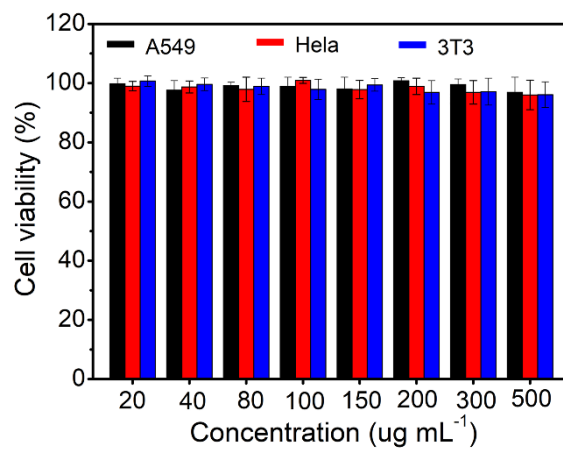


Fig. S30 Cells cytotoxicity of PLNP-BAC-PEGBT against A549, HeLa and 3T3 cells. Center values and error bars are defined as mean and s.d., respectively ($n = 5$).

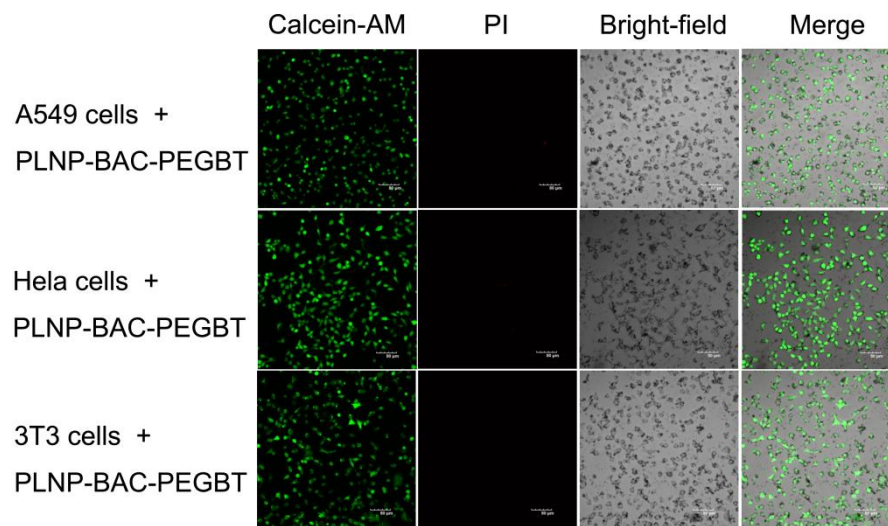


Fig. S31 Cells cytotoxicity of PLNP-BAC-PEGBT ($200 \mu\text{g ml}^{-1}$) against A549, HeLa and 3T3 cells (Calcein-Am and PI staining, scale bar, $80 \mu\text{m}$).

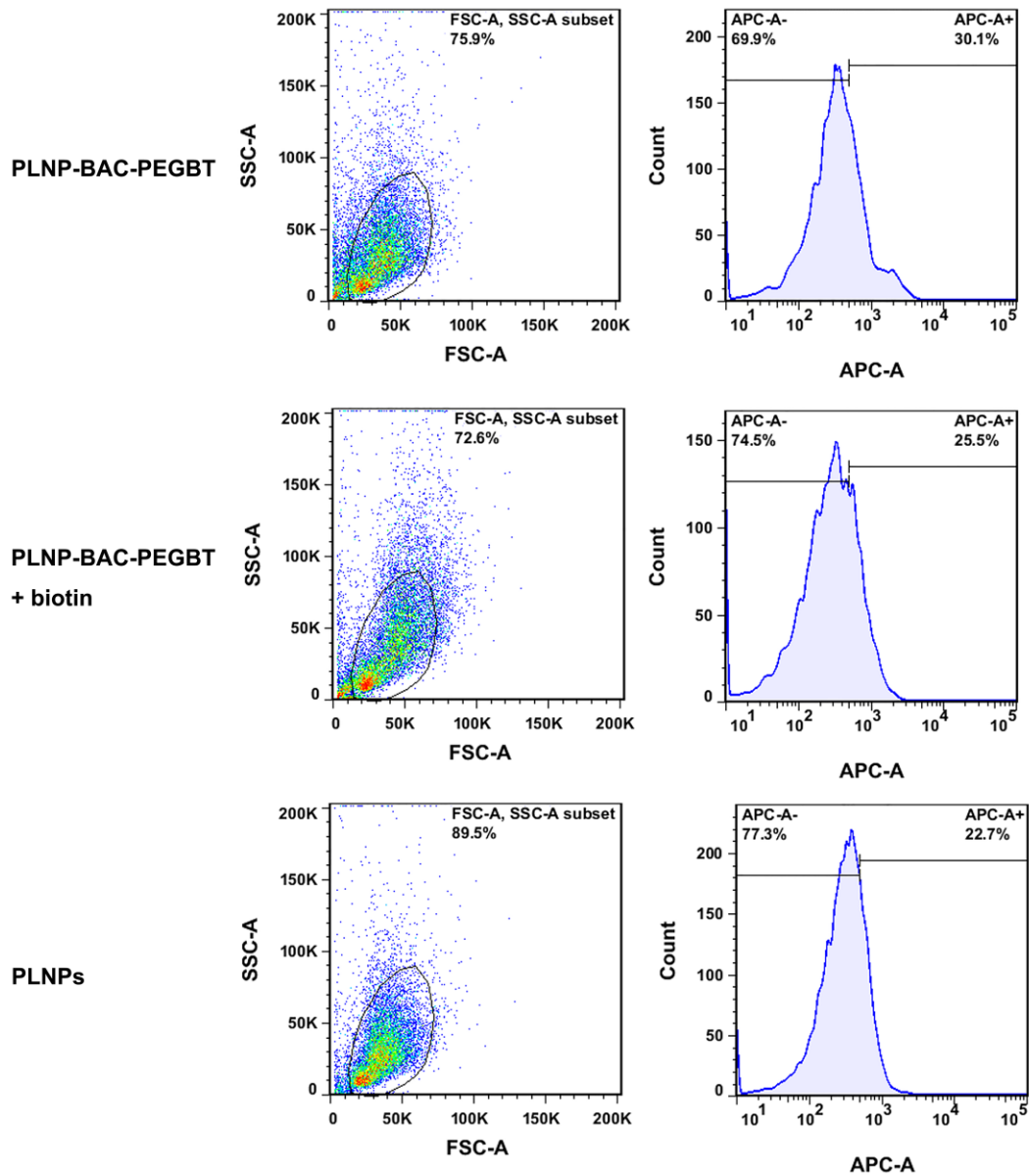


Fig. S32 Flow cytometry analysis of A549 cells (pre-treated with BT or not) after incubation with PLNP-BAC-PEGBT or PLNPs, respectively. The mean fluorescence intensity (MFI) obtained from flow cytometry show that the MFI in A549 cells incubated with PLNP-BAC-PEGBT was α . 1.4-times higher than that in A549 cells treated with PLNPs, further confirming the active targeting specificity of BT.

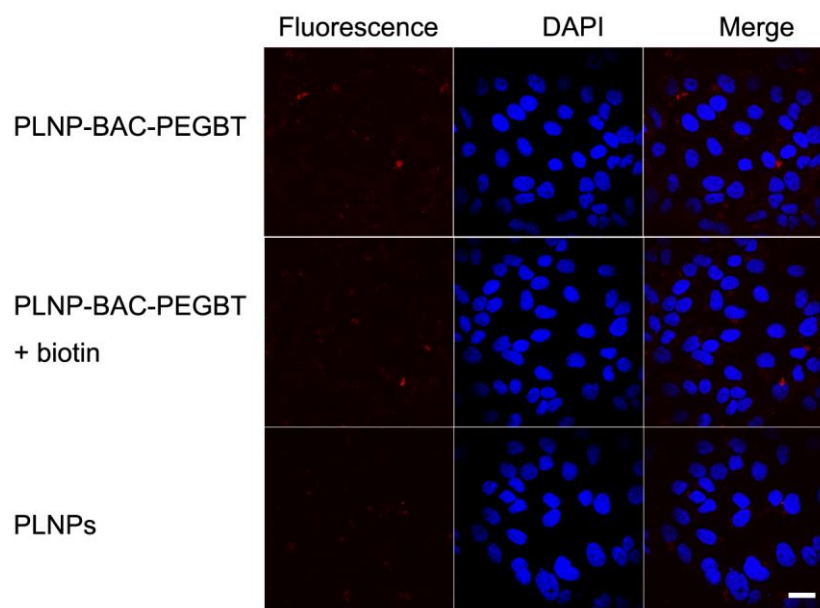


Fig. S33 Cell internalization and cell imaging of PLNP-BAC-PEGBT toward HeLa cells. Confocal laser scanning microscope (CLSM) imaging of HeLa cells pre-treated with biotin or not incubated with PLNP-BAC-PEGBT or PLNPs ($75 \mu\text{g mL}^{-1}$) (Scale bar, $30 \mu\text{m}$).

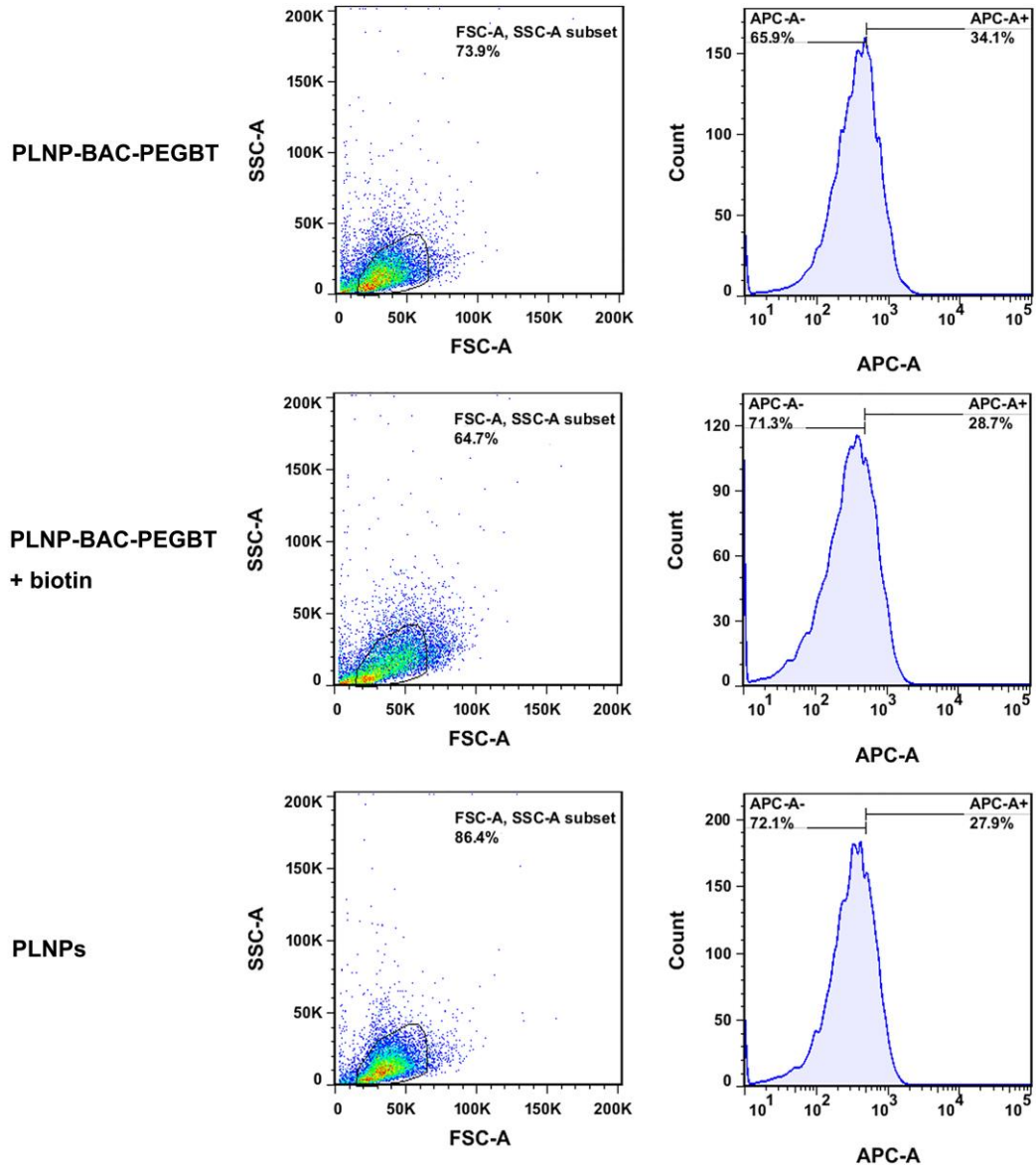


Fig. S34 Flow cytometry analysis of HeLa cells (BT per-blocked or not) treated with PLNP-BAC-PEGBT or PLNPs, respectively.

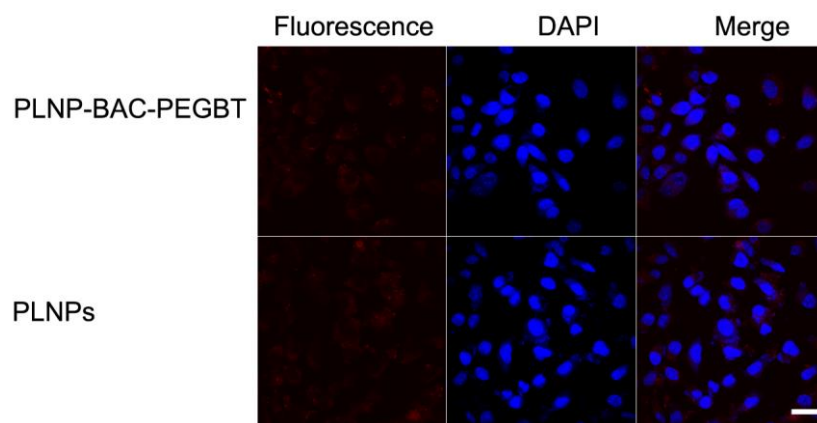


Fig. S35 Cell internalization and cell imaging of PLNP-BAC-PEGBT toward 3T3 cells. CLSM imaging of 3T3 cells incubated with PLNPs-BAC-PEGBT or PLNPs ($75 \mu\text{g mL}^{-1}$) (scale bar, $30 \mu\text{m}$).

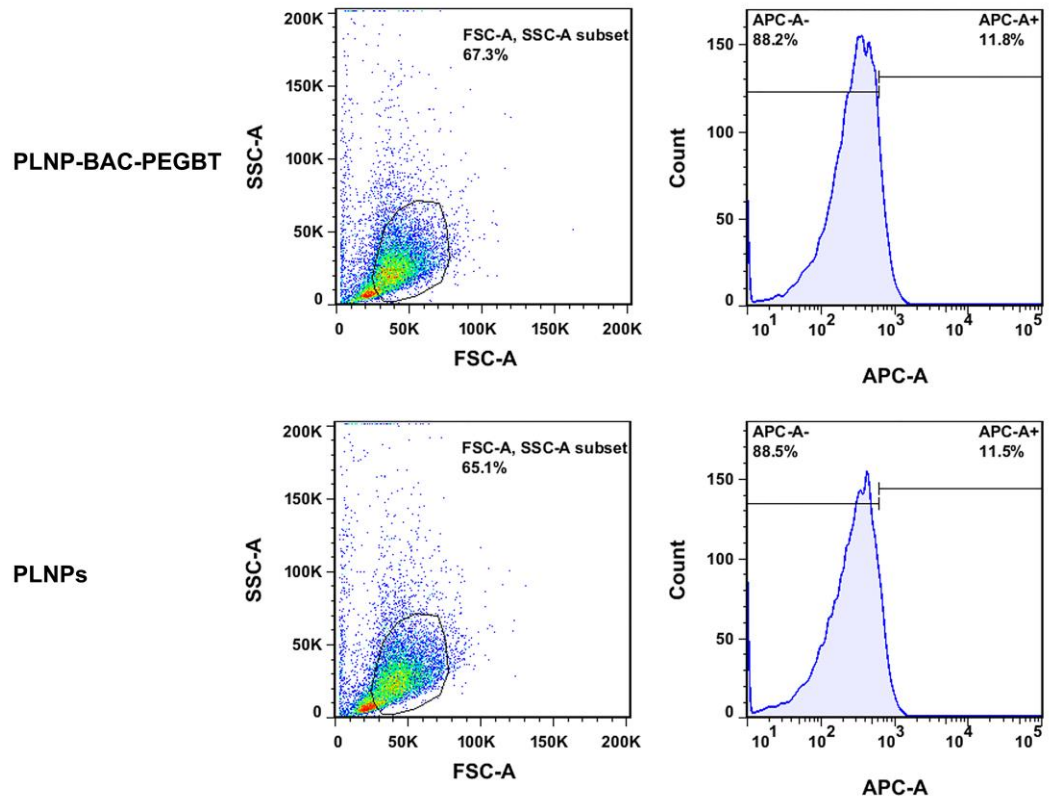


Fig. S36 Flow cytometry analysis of 3T3 cells incubated with PLNPs-BAC-PEGBT or PLNPs.

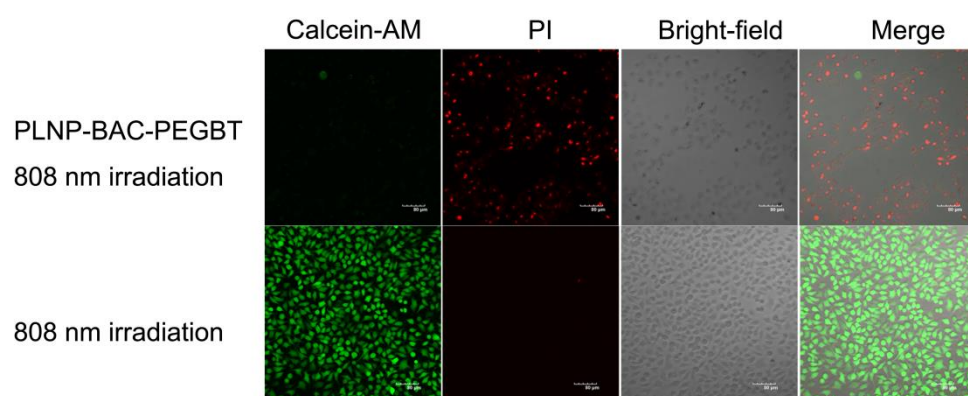


Fig. S37 Cell cytotoxicity of PLNP-BAC-PEGBT against Hela cells under 808 nm laser irradiation.

CLSM imaging of Hela cells incubated with PLNP-BAC-PEGBT ($75 \mu\text{g mL}^{-1}$) or not under 10 min of 808 nm laser irradiation (0.6 w cm^{-2}) (Calcein-Am and PI staining).

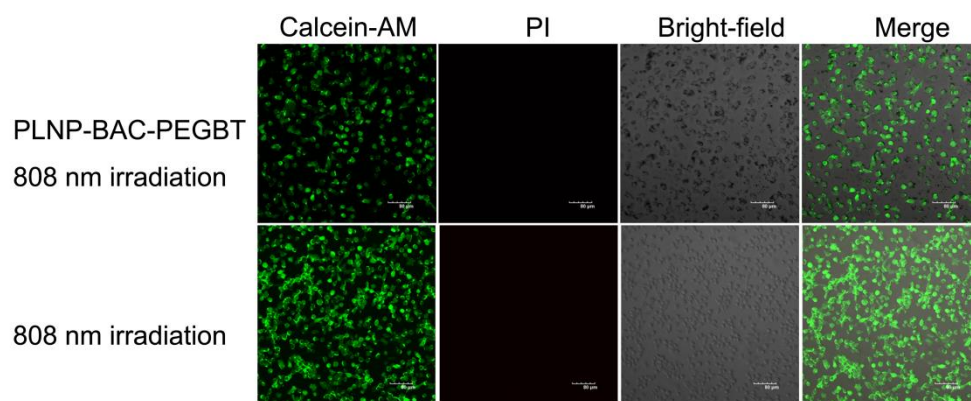


Fig. S38 Cell cytotoxicity of PLNP-BAC-PEGBT against 3T3 cells under 808 nm laser irradiation. CLSM imaging of 3T3 cells incubated with PLNPBAC-PEGBT ($75 \mu\text{g mL}^{-1}$) or not under 10 min of 808 nm laser irradiation (0.6 w cm^{-2}) (Calcein-Am and PI staining).

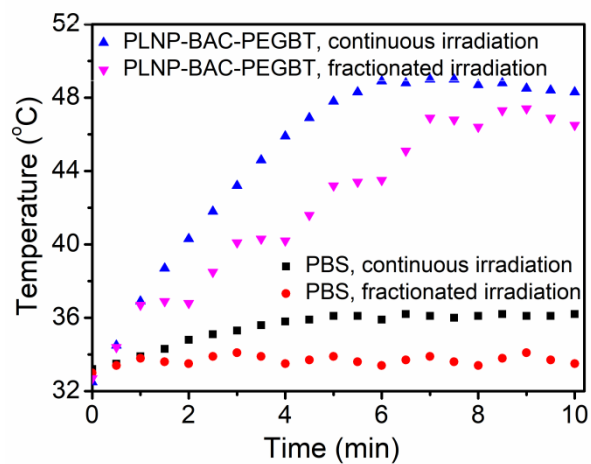


Fig. S39 PLNP-BAC-PEGBT or PBS-mediated *in vivo* photothermal effect: Temperature change of mice (tumor sites) subjected to continuous or fractionated (repeated cycles of 1 min laser on/1 min laser off) 808 nm laser irradiation (0.6 w cm^{-2} , for a total time of 10 min) after intravenous injection of PLNP-BAC-PEGBT (4 mg mL^{-1}) or PBS.

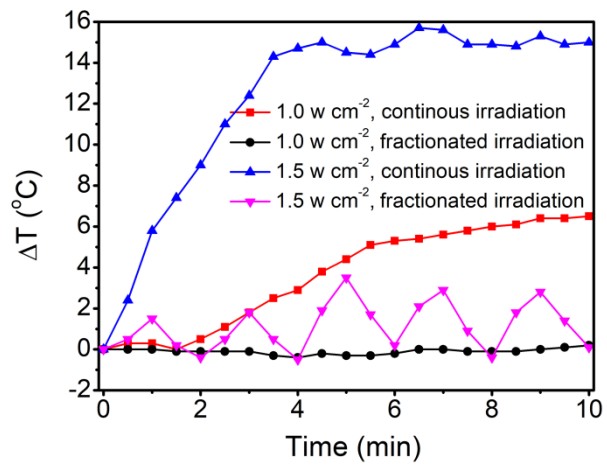


Fig. S40 Thermal effect of 808 nm laser itself. Temperature change of the mice treated with different powers of continuous or fractionated 808 nm laser irradiation.

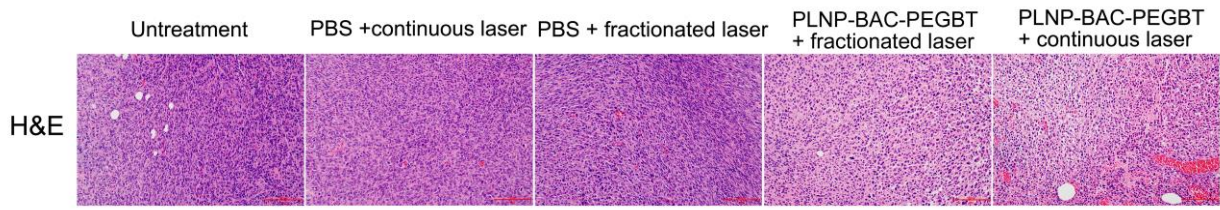


Fig. S41 H&E staining of tumor tissues of mice at 24 h post treatment (Scale bar, 100 μm).

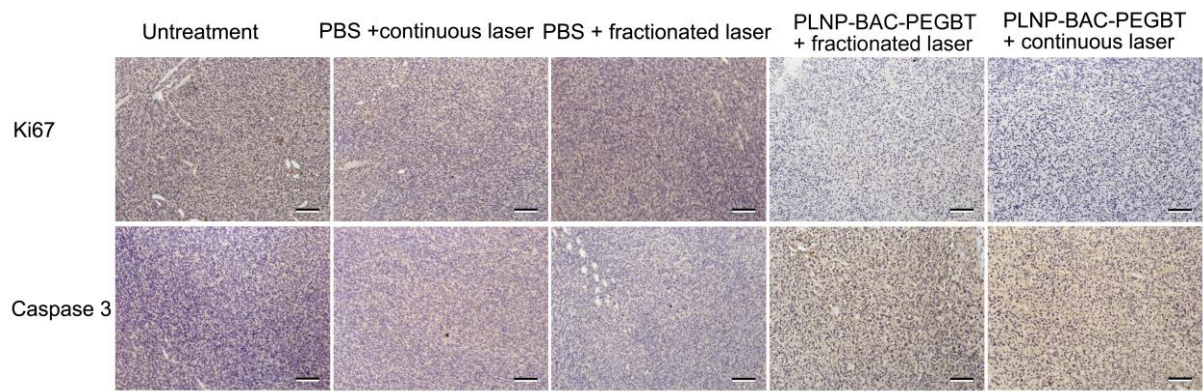


Fig. S42 IHC analysis of tumor tissues of mice at 24 h post treatment (Scale bar, 100 μ m)